Palaeogeography, Palaeoclimatology, Palaeoecology 511 (2018) 52–79

Contents lists available at ScienceDirect

Palaeogeography, Palaeoclimatology, Palaeoecology

journal homepage: www.elsevier.com/locate/palaeo

Mega-meander paleochannels of the southeastern Atlantic Coastal Plain, USA

Bradley E. Suther[a,*], David S. Leigh[b], George A. Brook[b], LinHai Yang[c]

[a] Department of Geography and Anthropology, Kennesaw State University, Kennesaw, GA 30144, United States
[b] Department of Geography, University of Georgia, Athens, GA 30602-2502, United States
[c] Key Laboratory of Desert and Desertification, Northwest Institute of Eco-environment and Resources, Chinese Academy of Sciences, Lanzhou 730000, China

ARTICLE INFO

Keywords:
Bankfull flow
Carolina
Climate change
Discharge
Georgia
Late Pleistocene

ABSTRACT

Paleodischarge estimates based on the slope-area method and channel boundaries determined from stratigraphic cross-sections indicate that large, terminal Pleistocene meandering paleochannels ("mega-meanders") in river valleys of the southeastern Atlantic Coastal Plain of the United States represent bankfull flows that were at least double the magnitude of those on modern rivers. Correlation of radiocarbon- and luminescence-dated paleomeanders with previously reported pollen and eolian sedimentary records suggests that greater discharge was driven by seasonally wetter conditions resulting from dynamic changes to regional precipitation and runoff that occurred in association with global warming at the end of the Pleistocene. While reflecting larger channel-forming flows, the exceptionally large widths and radii of curvature of mega-meanders were nonetheless maintained by a relatively modest discharge magnitude that was between two and four times larger than modern bankfull flow and within the size range of the present two- to five-year flood. Despite their large planform, the paleochannels conveyed relatively modest bankfull discharges because a wide, shallow shape limited their cross-sectional area and hydraulic radius. Within the late Quaternary evolution of fluvial systems in the region, scrolled mega-meanders constitute a transitional meandering planform that remained influenced by large volumes of sandy bedload following the sand-bed braided channels of the late Wisconsin interval, circa 30–17 ka. In addition to greater discharge, the large planimetric dimensions of paleochannels reflect a lack of cohesive vertical accretion facies on paleomeander floodplains, a sediment regime that transported large quantities of bedload sand, and the influence of these factors on channel boundary composition, bank stability, and channel shape. Findings underscore the importance of reconstructing channel cross-sectional dimensions and slope when estimating discharge for infilled paleomeanders. This approach reduces uncertainties surrounding channel cross-sectional area, gradient, and boundary composition inherent to studies lacking subsurface data that rely upon meander geometry to retrodict discharge.

1. Introduction

Many river valleys in the southeastern Atlantic Coastal Plain of the United States contain unusually large terminal Pleistocene and early Holocene meandering paleochannels ("mega-meanders") that exhibit channel widths, radii of curvature, and meander wavelengths approximately 2.0 to 5.0 times larger than those of late Holocene paleochannels and modern rivers in the region (Gagliano and Thom, 1967; Leigh and Feeney, 1995; Leigh, 2006; Leigh, 2008; this paper). Because in humid climates the planimetric and cross-sectional dimensions of alluvial channels are controlled in part by the discharge of low magnitude, high frequency (one- to five-year recurrence interval) floods, meandering paleochannels can be used to estimate past discharge (Dury, 1976; Knox, 1985; Williams, 1988; Carson et al., 2007). Regression equations that model paleodischarge based on relationships between discharge and channel width, radius of curvature, and meander wavelength established on modern, gaged rivers in the region indicate that mega-meanders may have conveyed channel-forming (bankfull) discharges that were 1.3 to 4.2 times larger than those of modern rivers (Leigh and Feeney, 1995; Leigh, 2006). Previous workers have used these paleodischarge estimates, along with fossil pollen records, to suggest that the terminal Pleistocene and early Holocene were times of greater runoff and (at least seasonally) wetter paleoclimate in the southeastern US (Leigh, 2006, 2008).

However, paleodischarge retrodiction based on planform meander dimensions alone may be subject to considerable inaccuracy (Rotnicki,

* Corresponding author.
E-mail address: bsuther@kennesaw.edu (B.E. Suther).

https://doi.org/10.1016/j.palaeo.2018.07.002
Received 2 October 2017; Received in revised form 30 June 2018; Accepted 4 July 2018
Available online 09 July 2018
0031-0182/

1991; Reinfelds and Bishop, 1998), which can result from a number of factors, including: misidentification of paleochannel boundaries on aerial imagery (Dury, 1976); use of paleohydrologic equations outside the range of their empirical limits (Williams, 1988); and large regression model standard errors (Dury, 1985). Although lower than the errors reported for more commonly applied paleohydrologic equations (Reinfelds and Bishop, 1998, p. 38), standard errors for the regionally-derived relationships of Leigh and Feeney (1995) used in previous studies of mega-meander channels are still relatively high, ranging from ± 43 to 53% of the modeled discharge for modern rivers in the Georgia and South Carolina Coastal Plain (see Eqs. 1–3 in Table 1 of Leigh and Feeney, 1995). These equations also face limitations with respect to application on channels of large Coastal Plain catchments, because they were developed using data from small to medium-sized rivers, with drainage areas of 700 to 15,000 km^2 and bankfull widths of three to 110 m (T. Feeney, personal communication, 2010). Such empirical constraints potentially reduce the accuracy of discharge estimates for the largest paleomeanders in the study area, which have respective basin sizes and bankfull widths in excess of 20,000 km^2 and 400 m. Given the limitations of previous investigations in the region, more reliable discharge estimates are needed if the late Quaternary paleohydrology of rivers in the southeastern Atlantic Coastal Plain is to be better understood.

The high standard errors typical of many paleohydrologic equations, including those previously applied to large paleomeanders within the southeastern Coastal Plain, probably reflect in part the failure of bivariate regression models to account for variables other than discharge that influence channel geometry (Bridge, 2003). This concern highlights a theoretical shortcoming of such "regime-based" paleohydrologic techniques, as the dimensions of alluvial channels are controlled not only by water discharge but also by sediment supply and size, bed and bank material, and bank vegetation (Knighton, 1998). Early work by Schumm (1960) recognized the influence of bed and bank material on channel morphology, indicating that the width to depth ratios of alluvial channels decrease as the silt and clay content of the channel perimeter increases and that this relationship occurs independent of changes in discharge. Other workers have observed similar relationships (Osterkamp, 1980; Simons and Albertson, 1963; Huang and Nanson, 1998). Findings from recent studies (Leigh, 2006, 2008) suggest such sediment-related channel-shape effects may have influenced the morphology of large paleomeanders in the southeastern Atlantic Coastal Plain. Leigh (2006) indicates that terminal Pleistocene meandering river channels in the region continued to transport large amounts of sandy bedload following an interval of late Wisconsin (30–16 ka) sand-bed channel braiding. Very sandy, scrolled point bars and thin vertical accretion deposits on terminal Pleistocene floodplains (Leigh, 2008) suggest that mega-meanders had sandier banks than late Holocene and modern channels and a sediment discharge regime that was more heavily influenced by bedload sand. This apparent difference in sediment load and channel boundary composition may have contributed to the unusually large widths, radii of curvature, and wavelengths exhibited by meander scars of the 17–11 ka interval in the study area. In light of these considerations, along with more precise paleodischarge estimates, it is clear that field-based stratigraphic investigation of large paleomeanders in the southeastern Coastal Plain is required if the factors responsible for their channel morphology are to be fully evaluated.

Large paleochannels that are morphologically similar to those of southeastern US Atlantic drainages are also found in the US Gulf Coastal Plain, where they occur in association with stratigraphic units of the "Deweyville Complex" along rivers from Texas to Mississippi (Autin et al., 1991; Blum and Aslan, 2006). The Deweyville units consist of successions of sand-dominated channel belts graded to lower sea-levels on the continental shelf and shelf edge that were associated with falling stage to lowstand intervals of the OIS 4–2 glacial period (Blum and Aslan, 2006; Sylvia and Galloway, 2006). Most recent studies argue that the Deweyville channels reflect climatic forcing mechanisms (Autin et al., 1991; Blum et al., 1995; Blum and Aslan, 2006; Sylvia and Galloway, 2006), but Blum and Aslan (2006) state that it is not yet possible to correlate the Deweyville paleochannels to specific paleoenvironmental conditions.

While a few previous studies have implied that large paleomeanders along rivers of the US Gulf and Atlantic Coasts might be considered as a group of correlative features under the "Deweyville" concept (Gagliano and Thom, 1967; Gagliano, 1991), more recent research from the Atlantic (Leigh, 2008) and Gulf (Blum and Aslan, 2006) Coastal Plains indicates that such generalized treatment of paleochannels from the southcentral and southeastern US is inappropriate. Large, scrolled paleomeanders of the Carolinas and southeastern Georgia differ from those of the Gulf Coast in that the Atlantic mega-meanders date to *terminal* OIS 2 and reflect channel adjustment that correlates closely to well-documented regional changes in vegetation and climate following sand-bed channel braiding during the OIS 3 and OIS 2 intervals (Leigh, 2006, 2008). Thus, rivers of the Gulf and southeastern Atlantic Coastal Plains appear to have experienced different Late Pleistocene evolutionary histories, and the view taken here is that the Deweyville paleomeanders represent channel forms produced by fluvial systems distinct from those in the Atlantic Coastal Plain that require separate study. Therefore, evaluation of the Deweyville paleomeanders of the US Gulf Coast is beyond the scope of this paper, and the present investigation focuses exclusively on paleochannels from the Atlantic Coastal Plain of Georgia and the Carolinas.

This study tests the hypothesis that mega-meanders of the southeastern Atlantic Coastal Plain conveyed larger-than-modern bankfull discharge using paleodischarge estimates that are based on field-surveyed paleochannel cross-sectional dimensions, estimates of paleochannel slope, and hydraulic modeling by the slope-area method. This paper also presents new radiocarbon and optically-stimulated luminescence (OSL) age estimates for four previously undated mega-meander paleochannels, along with stratigraphic data from closely spaced borings, that improve our understanding of the timing of mega-meanders in the southeastern US, the stratigraphy of their channel fills and paleo-floodplain deposits, and sedimentologic influences on their channel morphology.

Large paleomeanders of latest Pleistocene age (circa 19–11 ka) also occur in many other locations in the northern hemisphere, especially within the periglacial zone of the Last Glacial Maximum (LGM) in Europe (Sidorchuk, 2003; Starkel et al., 2015), where a pronounced snowmelt runoff season, high surface runoff from persisting permafrost, and low evapotranspiration were among factors that contributed to larger than modern bankfull discharges (Rotnicki, 1991; Kozarski, 1991; Howard et al., 2004; Sidorchuk et al., 2001; Borisova et al., 2006). However, regional pollen and eolian sedimentary records indicate LGM and terminal Pleistocene conditions in the southeastern US were more moderate than those of periglacial environments in Central and Eastern Europe. In a review of river response to late Quaternary climatic change in the region, Leigh (2008, see Table 2), notes that the southeastern Atlantic Coastal Plain during the late Wisconsin interval of 30–16 ka was very cold and dry relative to modern conditions, with January (winter) and July (summer) temperatures that respectively ranged from −1 to −10 °C and 15 to 20 °C. Annual precipitation was ≤400 mm/yr (Leigh, 2008); forest vegetation was sparse, consisting of jack pine and spruce interspersed with grasses and herbs (Watts, 1980); and conditions were sufficiently windy to transport much eolian sand on floodplains (Ivester et al., 2001; Leigh et al., 2004; Swezey et al., 2013), uplands (Swezey et al., 2016); and rims of Carolina bays (Ivester et al., 2007). In contrast, the terminal Pleistocene interval of 16–11 ka was cool and moist compared to the modern climate, with cold winters (January temperatures of 0 to −5 °C), mild summers (July temperatures of 20 to 25°), precipitation values of 800–1200 mm/yr, and a possible pronounced flood season (Leigh, 2008). Although periglacial processes may have operated for brief periods of time in the

mountainous headwaters of some rivers in the region, as suggested by block fields in the Blue Ridge Mountains (Hadley and Goldsmith, 1963) and possible solifluction deposits on the extreme upper Piedmont of North Carolina (Kerr, 1881), no clear evidence of Late Pleistocene periglacial conditions or continuous permafrost exists within the lower Piedmont or southeastern Coastal Plain (Leigh, 2008) where the majority of drainage area for the rivers examined in this study is located.

Given this context, mega-meanders of the southeastern Atlantic Coastal Plain are somewhat unusual relative to large paleochannels from more northerly locations, in that they occur in a present-day humid subtropical region that did not experience widespread periglacial landscape conditions or glacial meltwater runoff during the LGM or terminal Pleistocene. Thus, a final objective of this paper is to provide insights into the paleoenvironmental drivers that contributed to large meander development in this relatively low latitude setting, where climatic, hydrologic, and vegetation cover changes appear to have been more subtle than those experienced by rivers at higher latitudes.

2. Study area

2.1. Basin characteristics and geomorphic setting

Study sites include mega-meander paleochannels along the Oconee, Ogeechee, Congaree, Black, Pee Dee, and Neuse Rivers in the southeastern Atlantic Coastal Plain, USA (Fig. 1). With the exception of the Black River, these drainages head on the saprolite-mantled Paleozoic crystalline terranes of the Southern Blue Ridge or Piedmont provinces and flow across the Cretaceous and younger sediments of the Coastal Plain. For rivers originating in the Blue Ridge and Piedmont, headwaters respectively range in elevation from 500 to 1200 and 210–360 masl, while headwaters of the Black River, located in the upper Coastal Plain, have elevations of around 100–130 masl. Elevations of Coastal Plain uplands adjacent to Quaternary river valleys range from 20 to 30 masl in the vicinity of the Black River site in the lower Coastal Plain to around 100–140 masl near the Congaree River on the upper Coastal Plain. Along survey transects at field sites, mega-meander point bars have ground surface elevations that vary from 13 (Black R.) to 33 masl (Oconee R.).

Major rivers in the study area have basin sizes of 3000 to 36,000 km^2, with the largest drainages originating in either the Blue Ridge or Piedmont. Table 1 reports drainage areas and discharge estimates for modern river channels near mega-meander field sites and the nearest U.S. Geological Survey (USGS) gaging stations. For the Oconee, Congaree, Pee Dee, and Neuse Rivers, the majority of the drainage area upstream of study sites is contained within the Piedmont, while the drainage areas of the Ogeechee and Black River sites are respectively located either predominantly or entirely within the Coastal Plain. Sample sites were distributed among these six basins to provide a regional perspective on the paleohydrology of mega-meanders that reflects the physiography and range of catchment sizes typical of major rivers in the study area.

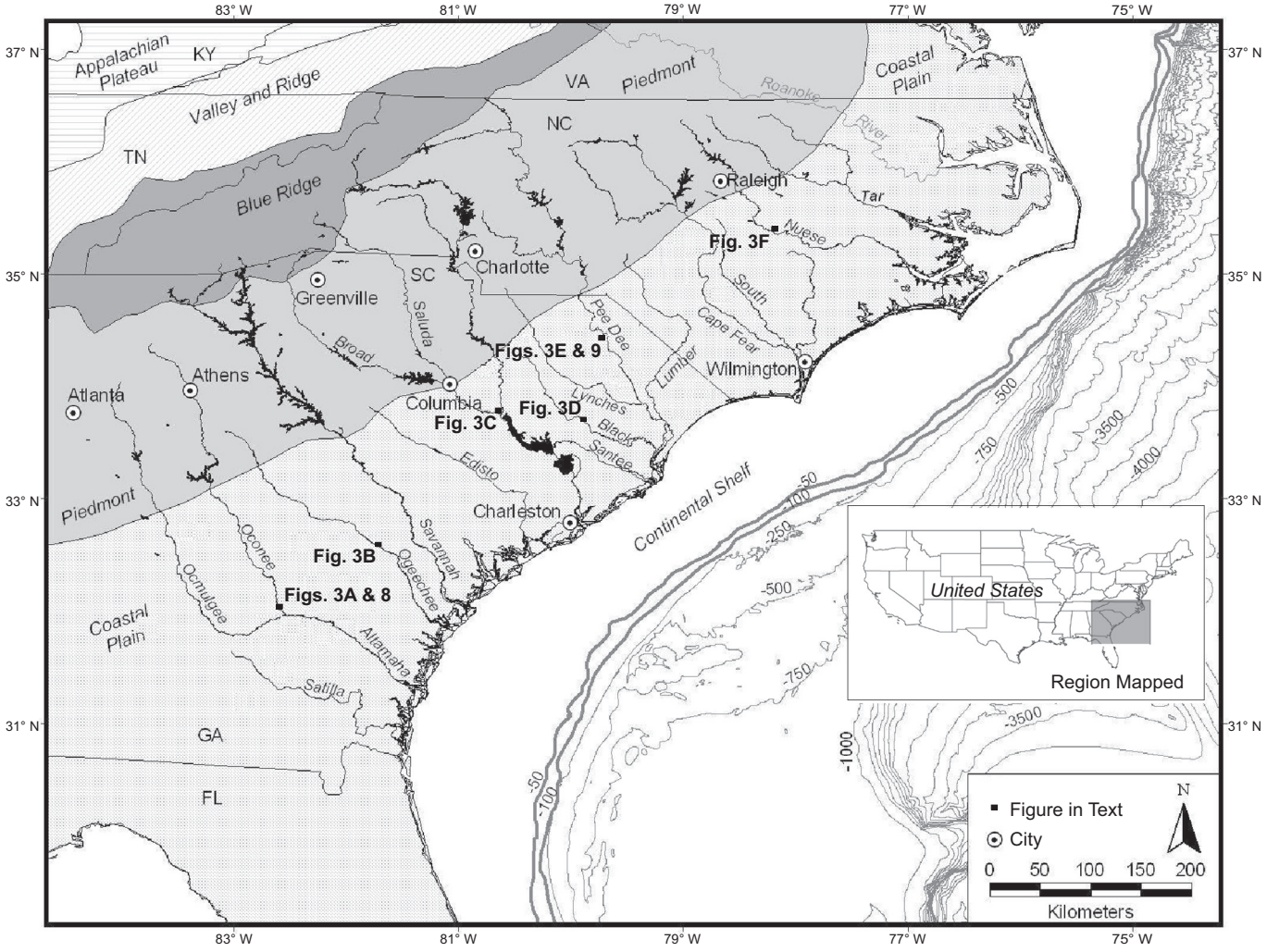

Fig. 1. Southeastern United States showing major rivers, physiographic regions, place names, and locations of study sites. The shallowest two bathymetric contour lines are placed at −50 and −100 m water depths to delineate the continental shelf. All other bathymetric lines are at 250 m intervals.

Table 1
Discharge estimates for modern rivers at mega-meander study sites and the nearest USGS gaging stations with ≥20 years of record.

River	Ungaged modern channels near mega-meander sites					Nearest USGS gaging station					
	Drainage area (km^2)	Discharge (m^3/s) predicted by regional flood frequency curves[a]		Weighted discharge (m^3/s)[a]		Gage name and number	Drainage area (km^2)	Discharge (m^3/s)[c,d]			
		Q_2	Q_5	Q_2	Q_5			$Q_{1.5}$	Q_2	Q_{maf}	Q_5
Oconee	13,736	799	1270	864	1388	Mt. Vernon, 02224500	13,235	639	828	903	1293
Ogeechee	5590	292	490	303	518	Scarboro, 02202000	5025	218	289	343	490
Congaree	22,062	1555[b]	2373[b]	–	–	Columbia, 02169500	20,332	2139	2789	3424	4746
Black	3032	166	289	150	289	Kingstree, 02136000	3243	98	139	205	283
Pee Dee	20,865	1450[b]	2215[b]	–	–	Pee Dee, 02131000	22,870	914	1138	1411	1835
Neuse	4928	422[b]	688[b]	360	555	Goldsboro, 02089000	6213	297	353	402	515

[a] Calculated using the *Flood-frequency applications tool for use on streams in Georgia, South Carolina, and North Carolina, Version 1.3*, (Gotvald et al., 2009b), based on the methods described in Gotvald et al. (2009a). Weighted discharge estimates discharge for a given recurrence interval flood based on the regional flood frequency curve and data from the nearest gage. Data required to calculate weighted discharge were not available for the Congaree and Pee Dee Rivers, so estimating weighted discharge for these sites was not possible. Q_2 and Q_5 = discharge of the 2- and 5-year flood as calculated by the Log Pearson Type III method, respectively.

[b] Present-day flood regimes of the Congaree, Pee Dee, & Neuse Rivers are regulated by impoundments. Thus, flood sizes derived from regional curves may not accurately reflect the post-impoundment regimes of these rivers. Reported discharges are intended as estimates of pre-dam flood sizes.

[c] $Q_{1.5}$ = discharge of the 1.5-year flood as calculated by the Log Pearson Type III method from the annual peak flood record at gaging stations. Q_{maf} = mean annual flood.

[d] Discharges were calculated for the pre-reservoir record for the Congaree (1892–1929, prior to completion of Lakes Murray & Greenwood; Feaster et al., 2009) and Neuse (1930–1980, prior to completion of Falls Lake; Weaver et al., 2009). The entire period of record for the Pee Dee at station #02131000 is regulated. Discharge estimates are based on water years 1939–1961, prior to completion of W. Kerr Scott & Tuckertown Reservoirs (Feaster et al., 2009). During this interval, flood storage capacity of all impoundments on the Pee Dee was approximately 40% less than its current value of $3.56 \times 10^8\ m^3$.

Modern rivers in the southeastern Atlantic Coastal Plain typically have single-thread, meandering channels with stable, cohesive, heavily vegetated banks and sand beds that are sometimes interspersed with gravelly riffles. In the vicinity of study sites, modern channels have slopes that range from < 0.0001–0.00032, sinuosities of 1.3–1.8, and bankfull widths that range from 25 to 55 m on the Black River to 100–190 m on the Congaree. The bedload of modern channels consists of sand and fine to medium gravel, but suspended load probably comprises the majority of the sediment load transported by Coastal Plain rivers with large drainage areas in the Piedmont (Meade et al., 1990). Modern floodplains are characterized by backswamp, oxbow, natural levee, and crevasse splay depositional environments and contain prominent fine-grained vertical accretion facies with weakly developed clayey to loamy soils in their upper parts. Meandering paleochannels with modern-like dimensions occur on the modern floodplain in the vicinity of all six mega-meander sites.

Fig. 2 provides a schematic surficial geologic map and cross-section that illustrate the typical geomorphic and stratigraphic contexts for mega-meander paleochannels in the study area. Map units in Fig. 2 are based on the findings of Leigh et al. (2004), Leigh (2006, 2008), Suther (2013), and this paper, and detail is provided for fluvial deposits of late Wisconsin and younger age (approximately 30 to 0 ka; units Qp2-Qh2). These units are depicted as informal alloformations (NACSN, 2005) and represent three-dimensional bodies of related lithofacies that can be differentiated based on bounding discontinuities. Paleochannel morphologies typically associated with Qp2-Qh2 are shown in Fig. 2 as surface morphological features.

Mega-meander deposits comprise an alloformation of mappable extent in most river valleys of the southeastern Atlantic Coastal Plain, represented by map unit Qp3 in Fig. 2. Surficial geologic mapping of the lower Oconee River valley near Uvalda, Georgia (Suther, 2013) indicates that this alloformation consists of normally graded alluvium composed of sandy lateral accretion and bedload lithofacies that are overlain by comparatively thinner, sandy to loamy overbank and clayey channel fill vertical accretion lithofacies (see map unit Qp6 of Suther, 2013, p. 41–45). At most sites, the geomorphic surface of the Qp3 alloformation constitutes a low terrace remnant 1 to 2 m higher than the modern floodplain and exhibits well-expressed to muted, sandy scroll bars (Figs. 2, 3A–F). In some localities, including the Damon mega-meander of the Pee Dee River (Fig. 3E), relict, eolian dunes occur on the scrolled topography and obviously were blown from the scroll bars (Leigh, 2008). Mega-meanders of the Qp3 surface are typically cross-cut into late Wisconsin braided channel deposits (Leigh et al., 2004), represented by the Qp2 alloformation in Fig. 2, or older Pleistocene fluvial deposits. Mega-meander paleochannels commonly contain cypress-gum swamp forests and are clearly evident as large meander scars on color-infrared aerial photography (Fig. 3) and satellite imagery.

2.2. Modern climate

The climate of the southeastern Atlantic Coastal Plain is classified as humid subtropical in the Köppen-Geiger system (Peel et al., 2007). Mean annual temperature and precipitation respectively range from 15 to 20 °C and 1100 to 1400 mm/yr. Summers are long and hot, and winters are mild with negligible snowfall. The study area receives rainfall throughout the year, though modes of higher precipitation occur during the winter months of January, February, and March (100–130 mm mean monthly totals), due to frontal precipitation from extra-tropical synoptic weather systems, and again in the summer months of July and August (120–200 mm mean monthly totals), as a result of tropical cyclones and localized, single-cell thunderstorms. The July–August mode in precipitation is most pronounced in the Coastal Plain because of the more direct influence of tropical storms and hurricanes on the region. Further inland in the neighboring Appalachian Piedmont province, monthly precipitation is more evenly distributed, with the highest amounts occurring in winter and early spring from frontal sources (January through April, 100–140 mm monthly totals). Flooding in the study area is typically induced either by extra-tropical synoptic systems during the winter and spring, when storm tracks are positioned closer to the region and evapotranspiration rates are low, or by inland precipitation from tropical storms and hurricanes during the summer and fall (Dobur and Noel, 2005). Native vegetation cover in the southeastern Atlantic Coastal Plain consists of deciduous, mixed, and southern pine forests and has been altered by agriculture, silviculture, and urbanization during historical time.

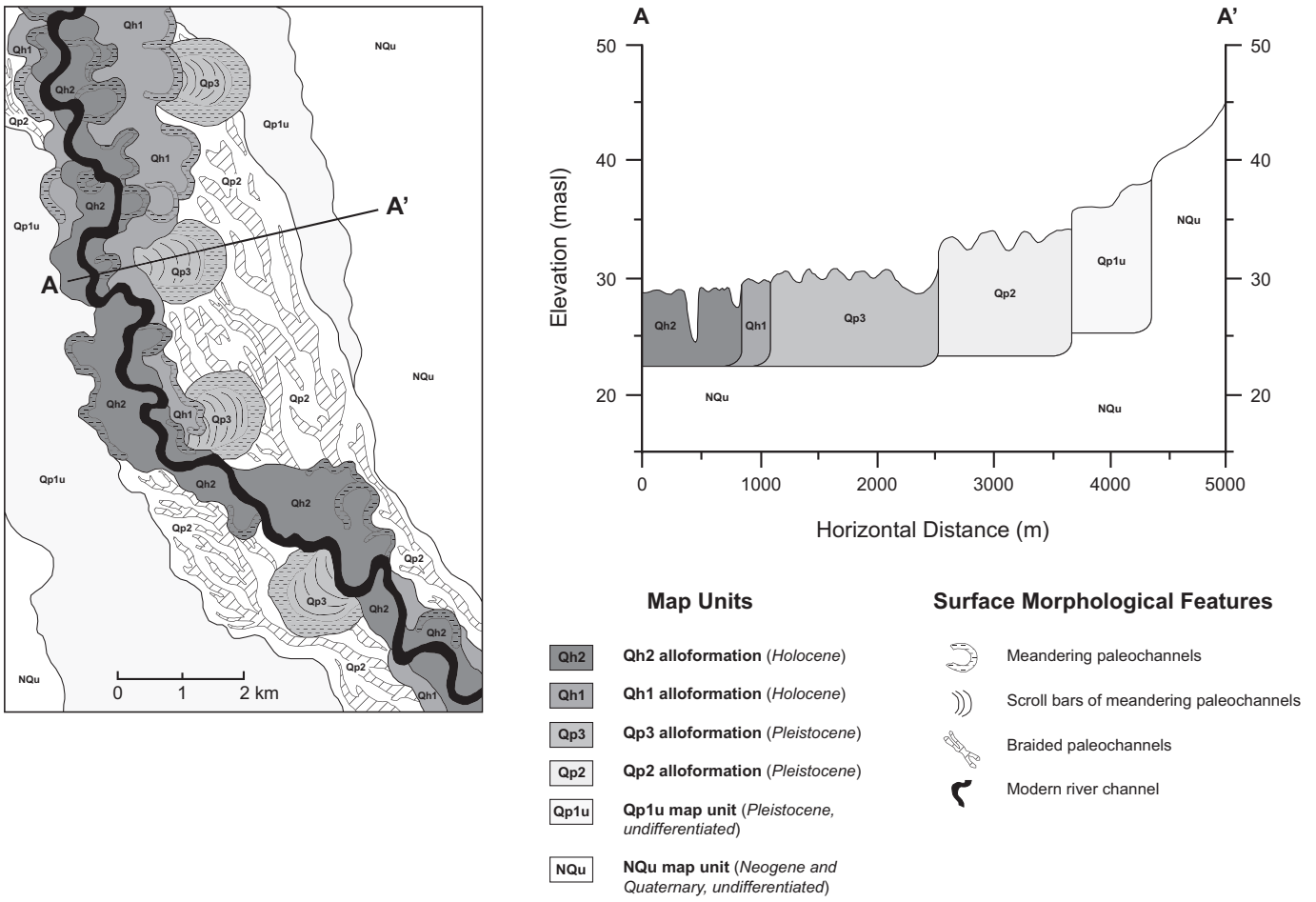

Fig. 2. Schematic surficial geologic map and cross-section illustrating the context of mega-meander paleochannels in river valleys of the southeastern Atlantic Coastal Plain, at locations > 60–80 km updip from the modern shoreline of the Atlantic Ocean. Mega-meander deposits constitute a mappable alloformation in most river valleys of the study area, depicted here as Qp3. The geomorphic surface of the Qp3 alloformation comprises the second terrace at most sites but is typically only 1–2 m above the modern floodplain. Qp3 is postdated by the Qh1 and Qh2 alloformations. Their surfaces respectively comprise the first terrace and floodplain in most settings and contain modern-sized meandering paleochannels. In some valleys, large paleomeanders occur on Qh1 that lack the pronounced scrollwork of Qp3 paleochannels (Leigh, 2008). Qp3 is immediately predated by the Qp2 alloformation, which consists of braided channel deposits of gravelly sand. The Qp2 surface typically corresponds to the third terrace and displays an interwoven pattern of braid bars and braided paleochannels. Eolian dunes (not shown) are common on braid plains of Qp2 and are also associated with scroll bars of the Qp3 surface in some places. Late Pleistocene braided and meandering channel deposits that predate Qp2 occur along many rivers and are here included with older fluvial sediments in a single map unit of undifferentiated Pleistocene alluvium (Qp1u). The NQu map unit consists of undifferentiated Neogene and Quaternary sediments of surrounding uplands, including Neogene Coastal Plain deposits that immediately underlie and laterally bound Quaternary alluvium at most sites.

2.3. Anthropogenic impacts to river channels

Over the past 200 years, rivers in the study area have experienced both indirect human impacts from land use change and direct impacts by impoundments. Pronounced indirect impacts in the form of historical land clearing and poor row crop farming practices caused upland soil erosion in the Piedmont portions of drainage basins, which increased water and sediment yield to rivers and resulted in regionally extensive floodplain vertical accretion of 0.5 to > 2.0 m (Happ, 1945; Trimble, 1974; Jackson et al., 2005; Walter and Merritts, 2008; Hupp et al., 2015). Upland soil erosion and increased stream sediment yields associated with post-colonial land use changes also occurred in the Coastal Plain (Phillips, 1993, 1997; Magilligan and Stamp, 1997). Few studies have explicitly addressed how historical increases in sediment supply have affected large river morphologies in the region. Brook and Luft (1987) suggest that elevated fine sediment inputs from agriculturally-driven erosion caused a small increase in sinuosity and decreases in radius of curvature and meander wavelength on the lower Oconee River. Hupp et al. (2015) report that sedimentation between 1725 and 1850 CE formed high banks and large levees along the upper and middle reaches of the Roanoke River in North Carolina, and that the modern channel has since incised through these sediments into underlying Coastal Plain deposits.

Among the drainages evaluated in this paper, the Ogeechee and Black Rivers are not impounded, while the Oconee, Congaree, Pee Dee, and Neuse Rivers are each regulated by one or more upstream dams (Gotvald et al., 2009a; Feaster et al., 2009; Weaver et al., 2009). The typical outcome of many large dams in the eastern United States has been a reduction in annual peak discharges (Graf, 2006) and an increase in minimum flows (Magilligan and Nislow, 2005). However, on two of the four regulated rivers examined here, the Oconee and Congaree, impoundment has had little impact on the size of high frequency (two-, five-, and 10-year return interval) peak flows that are of interest to the present study (Hess and Stamey, 1992; Conrads et al., 2008). Despite significant changes to water and sediment delivery, Leigh (2008) notes that the magnitude of historical channel change to large rivers in the region has been small in comparison to morphological differences exhibited by Late Pleistocene channels versus late Holocene and modern forms. The extent to which anthropogenic impacts influence paleo versus modern channel interpretations is evaluated in Section 5.4.

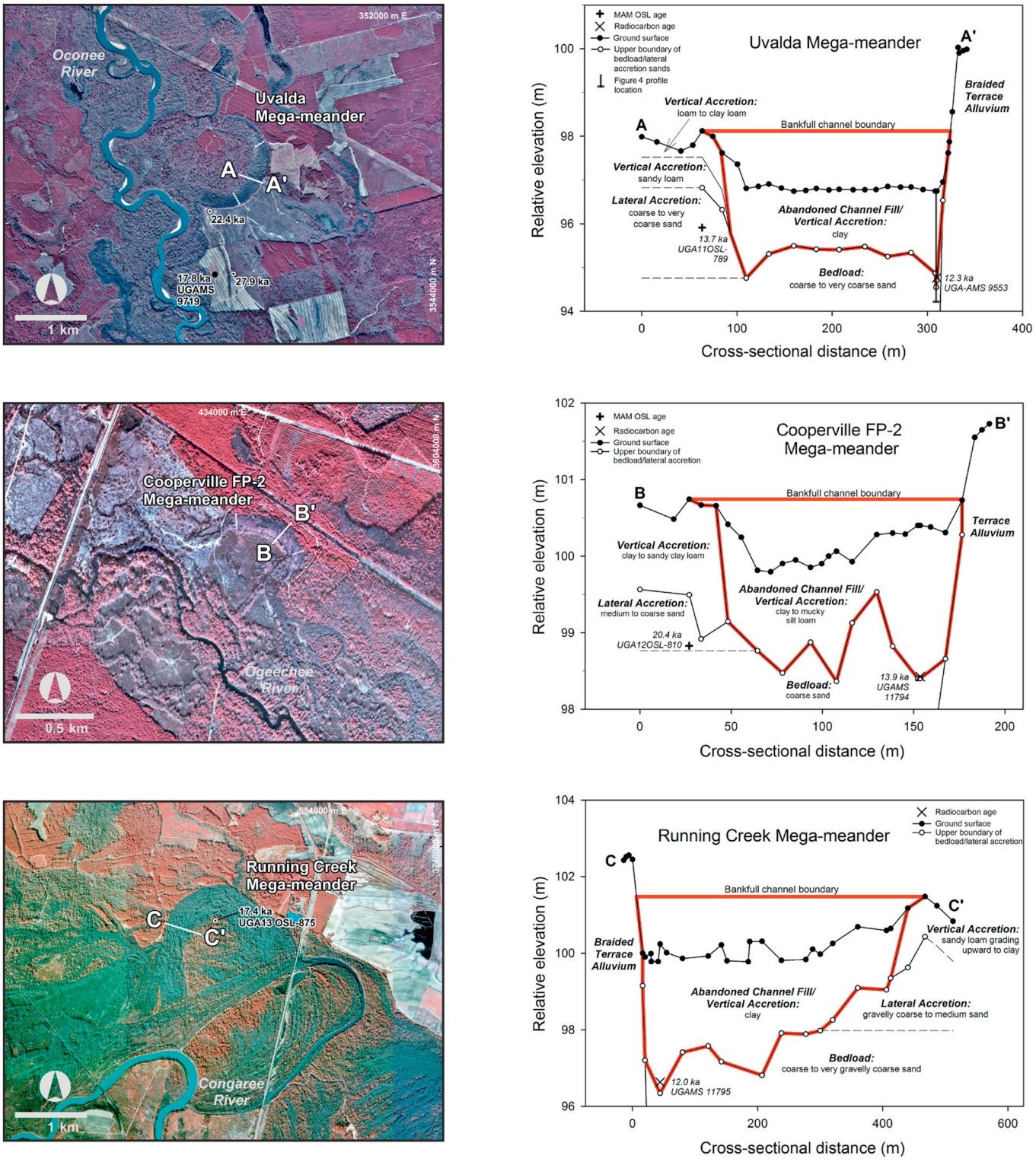

Fig. 3. Planimetric views and stratigraphic cross-sections of the (a) Uvalda (Oconee R.), (b) Cooperville FP-2 (Ogeechee R.), (c) Running Creek (Congaree R.), (d) Mouzon (Black R.), (e) Damon (Pee Dee R.) and (f) Moccasin Creek (Neuse R.) mega-meanders. Additional cross-sections used to estimate paleochannel slope for the Uvalda, Cooperville FP-2, and Moccasin Creek mega-meanders are shown with dashed lines on the planimetric figures for those sites. Radiocarbon (this paper) and OSL (Leigh et al., 2004) ages obtained from the braided terrace into which the Uvalda mega-meander is cross-cut are respectively represented by black and white circles on the aerial image. The Running Creek mega-meander OSL date (17.4 ± 2.2 ka) is located off the stratigraphic cross-section and shown on the planview diagram. For the Damon mega-meander, radiocarbon and OSL dates of Leigh et al. (2004) were projected a short distance from their true locations onto the E-E' section line and depicted on the stratigraphic cross-section. The blurred appearance of the Damon scrollwork results from eolian reworking of scroll bars, and the position of a 15.0 ± 1.4 ka OSL date obtained by Leigh et al., 2004 from a parabolic dune overlying scroll bar sediments at this locality is given on the aerial image for reference. Base maps for the planimetric figures are 1 m color infra-red digital orthophotographs registered to the North American Datum of 1983 and UTM grid zone 17. The inset map of the Moccasin Creek site shows a 1/9 arc-second (3 m) National Elevation Dataset digital elevation model of the paleomeander in the vicinity of its apex. Dashed lines on the inset map represent the lateral boundaries of the paleochannel ground surface.

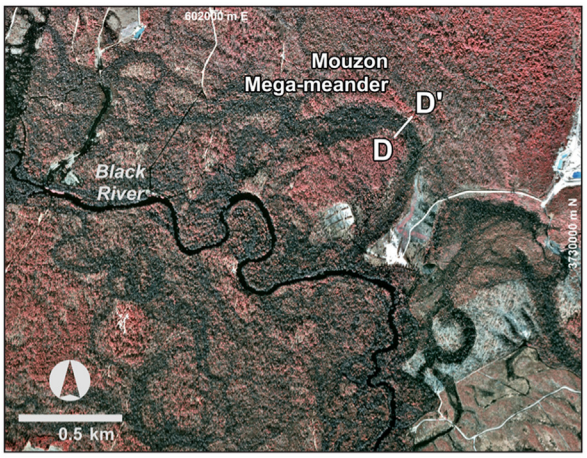

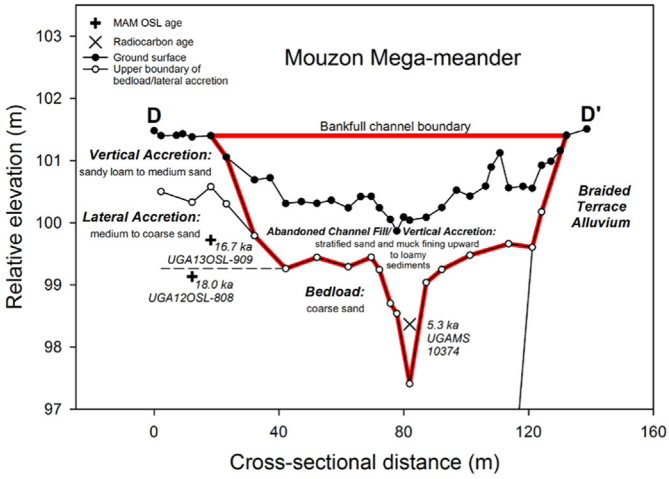

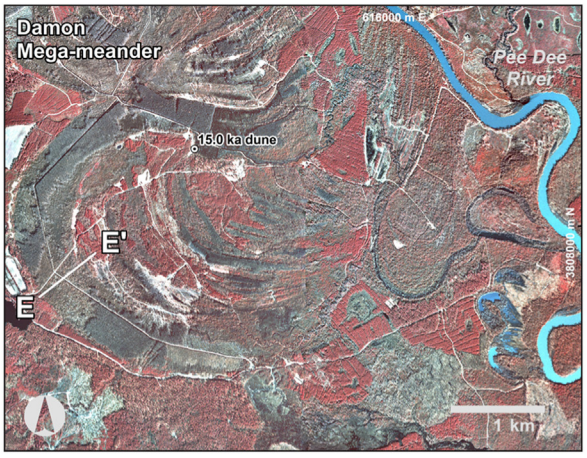

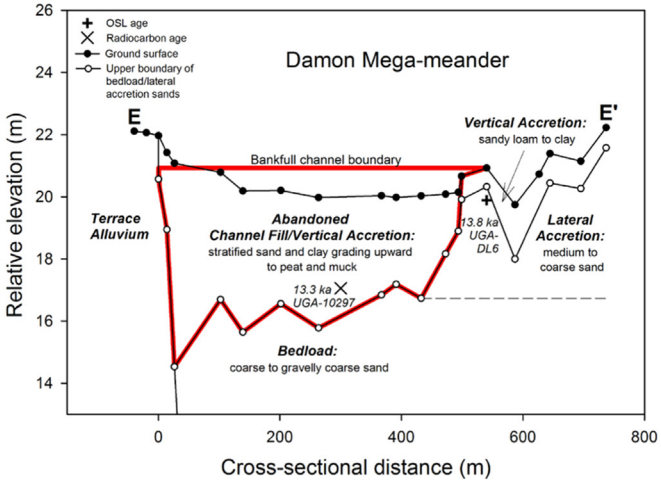

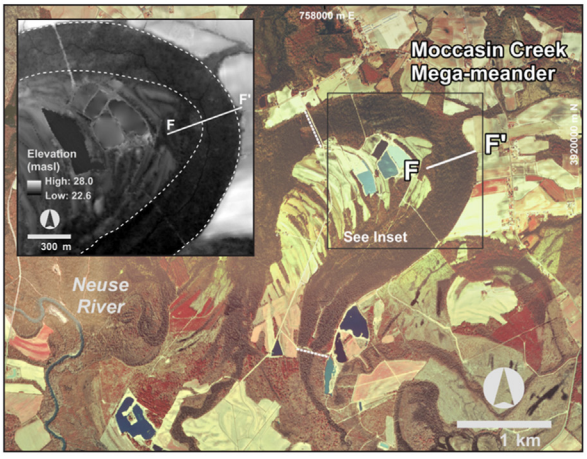

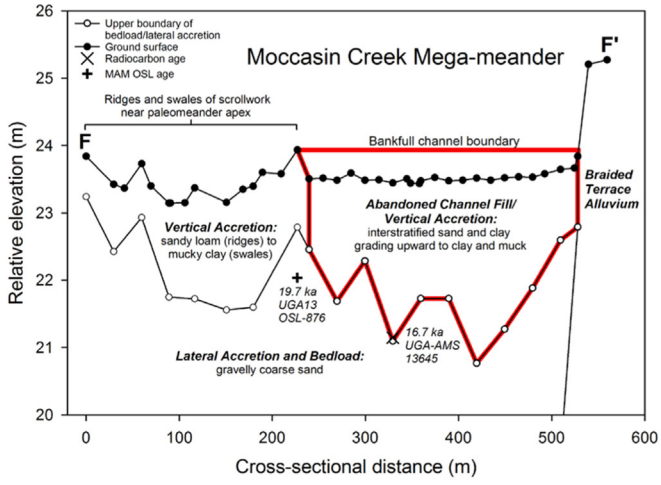

Fig. 3. (*continued*)

3. Methods

3.1. Paleodischarge estimation

Six well expressed, large meandering paleochannels with planform dimensions typical of mega-meanders in their respective valleys were identified on 1999 USGS color-infrared digital orthophoto quarter quadrangles and Landsat imagery. Mega-meander discharge was estimated by the slope-area method, which relies on flow resistance formulae, channel cross-sectional area, and slope (Whiting, 2003). Discharge was calculated using the product of channel cross-sectional area and average flow velocity determined by the Manning equation (Knighton, 1998):

$$v = R^{2/3}\, s^{1/2}/n \quad (1)$$

where v = velocity; R = hydraulic radius (channel cross-sectional area

divided by wetted perimeter); s = slope of the energy gradient; and n = Manning's roughness coefficient.

Cross-sectional area was determined for each mega-meander from channel boundaries delineated by stratigraphy observed along boring transects, using the following procedure modified from that of Knox (1985). Transects were situated near the apex of meander bends and oriented perpendicular to paleo-flow direction. Borings were spaced at intervals no coarser than one-tenth of channel width, and sampling was performed with either a bucket auger or Russian corer. In cases where the stratigraphy of paleochannel fill was fairly uniform, a steel tile probe was used in conjunction with borings to measure the depth to the contact between fine-grained channel fill sediment and channel bed sand. Morphological characteristics of soils and sediment were described according to USDA Soil Survey terminology (Soil Survey Division Staff, 1993), and lithologic properties and stratigraphic contacts were noted. Where present, organic materials were described as either peat, if plant forms were identifiable within the material, or as muck, if materials were so decomposed that identification of plant forms was not possible (USDA-NRCS, 2016). Ground surface elevations along transects were surveyed with an electronic total station or a rotary laser level.

One representative stratigraphic section from a typical large paleomeander, the Uvalda mega-meander of the Oconee River, was selected for detailed laboratory analysis to illustrate the sedimentological characteristics of paleochannel bed material versus those of younger paleochannel fill. The stratigraphic section was sampled by hand auger from the estimated thalweg position of the Uvalda mega-meander and analyzed in approximately 5 cm depth increments. Grain size analysis was performed using the modified pipette procedure of Indorante et al. (1990) and the sieve method (Ingram, 1971). Mass loss-on-ignition (LOI) was determined after heating samples for 5 h at 550 °C in a muffle furnace, to ensure complete combustion of organics (Heiri et al., 2001). To facilitate comparisons between paleo and modern channel bed sediments, grain size determinations by the pipette and sieve methods were also conducted on representative samples of bedload from the modern Oconee River.

Paleochannel slope was estimated using field-surveyed, paleochannel bed elevations for the Oconee, Ogeechee, and Neuse River mega-meanders, or was derived from the longitudinal gradient of the Qp3 alloformation's geomorphic surface (Congaree, Black, and Pee Dee River sites). Field-measured slopes were calculated from channel bed elevations along the main cross-sectional coring transect and along upstream and downstream cross-sections that were surveyed by the methods described above. The longitudinal gradient of the Qp3 geomorphic surface at each sampling locality was calculated using the tops of prominent mega-meander scroll bar ridges identified on either 2 or 3 m horizontal resolution LIDAR elevation data (Ogeechee, Congaree, Black, Pee Dee, and Neuse sites) or by using the prevailing treads of Qp3 surfaces identified on USGS 7.5-minute topographic quadrangles, where LIDAR data were unavailable (Oconee site). To account for meandering, a sinuosity of 1.7, derived from well-preserved mega-meander paleochannels on the Ogeechee and Black Rivers of one to greater than three wavelengths, was applied to all Qp3 valley gradients to better approximate channel slope. To account for uncertainty in slopes derived from valley gradients, the longitudinal gradient of the Qp3 surface was used as a maximum estimate, while the sinuosity-corrected gradient served as a minimum estimate. To bracket uncertainty in field-measured channel bed slopes, estimates calculated from elevations of the predominant surface and the lowest 20% of the channel bed were employed. Justification for the use of these channel bed components is provided in Section 4.2.

Manning's roughness coefficient (n) values for mega-meander paleochannels were estimated using the procedure of Arcement and Schneider (1989, pp. 2–8), which relies on Cowan's (1956) method for computing channel roughness, the base roughness values reported by Benson and Dalrymple (1967) for specific bed sediment sizes, and the n adjustment values of Aldridge and Garrett (1973). A base n value appropriate for sand-bed channels, with a bed sediment median grain size representative of mega-meanders, was added to incremental roughness values that accounted for effects of vegetation, variation in channel cross-section, and bank irregularities. The summed values were then multiplied by a correction factor for channel sinuosity.

Individual components of channel roughness were either measured directly or estimated. Paleochannel bed sediment size was determined in the laboratory by pipette and sieve analysis (Uvalda mega-meander) or in the field with a grain scale (all other sites). Sinuosity estimates were based on the same Black and Ogeechee River paleochannel measurements that were used in the slope estimation procedure (described above). Roughness contributions from vegetation were inferred from fossil pollen and eolian sedimentary records. Regional pollen sections indicate mega-meanders were active during a period of cool mixed to temperate deciduous forest cover (Watts, 1980; Hussey, 1993; Webb et al., 2004; LaMoreaux et al., 2009), but relict eolian dunes blown from the scroll bars of some mega-meanders suggest paleochannels may have lacked vegetation on their point bar sides (Leigh, 2008). Therefore, contributions to Manning's n values from paleovegetation were adjusted to reflect lower than modern riparian vegetation density. Roughness contributions from cross-section variation and non-vegetative bank irregularities were assessed at paleomeander sites with three field-surveyed cross-sections per paleochannel (Oconee, Ogeechee, and Neuse), and results were used to inform estimates of n value contributions from these sources across all six sites.

Because paleochannels are now infilled with sediment and their roughness cannot be precisely known, a best estimate (0.038) and range (0.030–0.045) of Manning's n values were computed for use in paleodischarge calculations, based on the factors described above. The range of n values reflects uncertainties associated with roughness contributions from paleovegetation, bank irregularities, and variation in paleochannel cross-sections and sinuosity.

Discharge estimates by the slope-area method typically have a percentage uncertainty of 10–20% at the 95% confidence level (p. 509, Herschy, 1985). To evaluate the reliability of this technique on alluvial rivers in the southeastern US, bankfull discharge was estimated at four USGS gaging stations in the Georgia Coastal Plain using field-surveyed cross-sections provided by the USGS South Atlantic Water Science Center in Georgia and slope estimates obtained from the best available elevation mapping. Ratios of slope-area to gaged estimates of bankfull discharge range from 0.96–1.24 (Table 2) and are generally consistent with the envelope of error expected for the slope-area method. These results indicate that this technique yields reasonable bankfull discharge estimates for modern rivers in the study area and lends credence to the paleodischarge estimates for paleochannels presented in this study. For all paleomeanders, a best estimate and minimum and maximum values for discharge are reported that reflect the best estimate and associated uncertainties for channel roughness and slope.

3.2. Radiocarbon and optically-stimulated luminescence (OSL) dating

To best approximate the timing of channel abandonment, samples for radiocarbon dating were collected at or near the thalweg of paleochannels from unoxidized, basal channel fill located immediately above channel bed sand. Only uncarbonized plant macrofossils (e.g., seeds, nuts, leaves) that appeared fresh and not reworked by fluvial transport were used. All radiocarbon samples were measured by the accelerator mass spectrometry method (AMS) at the University of Georgia (UGA) Center for Applied Isotope Studies following an acid-alkali-acid (HCl-NaOH-HCl) pretreatment. Radiocarbon dates were calibrated to calendar years with the CALIB 7.1 radiocarbon calibration program, using the IntCal 13 calibration curve (Stuiver et al., 2016).

Optically-stimulated luminescence (OSL) dating of paleomeander alluvium was conducted to provide additional age control for paleochannels. At each site, samples for OSL dating were obtained from

Table 2
Bankfull discharge estimates at selected gaging stations in the Georgia Coastal Plain using the slope-area method and comparison with discharges calculated from gage records.

River name and USGS gage #	Drainage area (km^2)	W/D[a]	CSA[b] (m^2)	WP[c] (m)	R[d]	Slope[e]	Manning's n[f]			Velocity (m/s)			Q_{BKF} (m^3/s) by slope-area[g]			Discharges calculated from gage records (m^3/s)[h]				
							Min	Max	Best estimate	Min	Max	Best estimate	Min	Max	Best estimate	Q_{BKF}	Slope area/ gaged Q_{BKF}	Q_{BKF} recurrence interval (yr)	$Q_{1.5}$	Q_2
Ogeechee near Eden, #02202500	6864	25.6	221.0	77.1	2.9	0.00014	0.030	0.040	0.035	0.59	0.78	0.67	130	173	**148**	**119**	**1.24**	1.07	231	303
Oconee at Dublin, #02223500	11,396	20.0	511.2	112.2	4.6	0.00019	0.030	0.040	0.035	0.94	1.26	1.08	481	642	**550**	**571**	**0.96**	1.36	649	849
Ocmulgee at Lumber City, #02215500	13,416	32.2	515.8	133.1	3.9	0.00020	0.030	0.040	0.035	0.86	1.15	0.99	445	593	**508**	**496**	**1.03**	1.37	554	724
Altamaha near Baxley, #02225000	30,044	46.4	857.1	217.7	3.9	0.00014	0.030	0.040	0.035	0.75	1.00	0.85	640	853	**731**	**639**	**1.15**	1.12	1109	1462

[a] Width to depth ratio.
[b] Cross-sectional area.
[c] Wetted perimeter.
[d] Hydraulic radius.
[e] Slope was measured from USGS 7.5-min topographic quadrangles for all gages except the Ogeechee River near Eden, where National Elevation Dataset 3 m horizontal resolution LIDAR data were used.
[f] Manning's roughness coefficient (n) values were estimated by criteria specified in Arcement and Schneider (1989) and by visual comparison with the viewbook of Barnes (1967).
[g] Bankfull discharge calculated by the slope-area method.
[h] Ratios of slope-area to gaged bankfull discharge, as well as the slope-area best estimates and gaged values used to calculate discharge ratios, are given in bold. Bankfull discharge at gage locations was estimated using a discharge-stage rating curve constructed by the authors from gage data and inspection of field-surveyed channel cross-sections obtained from the USGS South Atlantic Water Science Center-Georgia. $Q_{1.5}$ and Q_2 respectively indicate the discharge of 1.5- and 2-year recurrence interval floods calculated by the Log Pearson Type III method. The Oconee River is slightly entrenched in the vicinity of the Dublin, Georgia gage. This results in a bankfull flood discharge and recurrence interval that are greater at Dublin than at the Mount Vernon, Georgia gage, which is located ~60 km downstream in closer proximity to the Oconee mega-meander field site (Table 8).

lateral accretion or upper bedload sediment, beneath the scroll bar immediately adjacent to the paleochannel that functioned as the active point bar shortly prior to the time of channel abandonment. OSL samples were collected by pounding a light-tight metal tube with length by diameter dimensions of 30 × 7 cm into the base of a hand-augered hole. Immediately following sample collection, ends of tubes were sealed to prevent exposure to light. In all cases, samples for OSL dating were obtained from unweathered (C horizon) quartz-rich sand that lacked stratigraphic or pedogenic evidence of post-depositional mixing.

OSL dating was conducted at the University of Georgia Luminescence Dating Laboratory in subdued red-light conditions. Luminescence measurements were performed on sediments from the central sections of metal sample tubes, which were protected from light exposure during sampling. Raw samples were treated with 10% HCl and 20% H_2O_2 to remove carbonate and organic matter. After drying, samples were sieved to obtain grains in the 125–250 or 125–180 μm size range. Heavy liquids with densities of 2.62 and 2.75 g/cm^3 were then used to separate the quartz from feldspar grains in these size fractions. The quartz grains recovered were treated with 40% HF for 60 min to remove the outer layer irradiated by alpha particles and any remaining feldspar grains. They were then treated with 10% HCl for 10 min to remove fluorides created during the HF etching. The purity of quartz was checked by IRSL at 50 °C, and results showed that none of the samples contained feldspar in the quartz fraction. Large aliquots of purified quartz grains were then mounted on stainless steel disks with a diameter of 9.6 mm using silicone oil for OSL measurements.

OSL measurements were made using an automated Risø TL/OSL-DA-15 Reader (Markey et al., 1997). Stimulation was carried out by a blue LED (λ = 470 ± 30 nm) stimulation source for 60s at 125 °C. Detection optics were comprised of two Hoya 2.5 mm thick U340 filters and a 3 mm thick stimulation Schott GG420 filter coupled to an EMI 9635 QA photomultiplier tube. Laboratory irradiation was performed using a calibrated $^{90}Sr/^{90}Y$ beta source mounted within the reader.

The equivalent dose (D_e) was measured using a routine single aliquot regenerative-dose (SAR) protocol (Murray and Wintle, 2000), with a preheat temperature of 260 °C and a cut heat temperature of 220 °C. For D_e determination, dose-response curves were constructed using three regenerative dose points, a zero-dose point, and a repeat point. The initial OSL signals integrated over the first 1 s (1–2 channels) were subtracted by 'early background' (3–10 channels) to avoid a contribution of medium and slow components (Cunningham and Wallinga, 2010). For each sample, typically 24 aliquots were measured. Among the measured aliquots, any that exceeded the acceptable range for the recycling ratio (0.9–1.1) and recuperation (5%) were excluded from the D_e calculation.

Dose rate is caused by the radioactive elements existing in grains of the sample and surrounding sediments, and a generally lesser contribution from cosmic rays. A thick source Daybreak alpha counting system was used to estimate U and Th for dose rate calculations. Potassium was measured by ICP90 at the SGS Laboratory in Toronto, Canada, using the sodium peroxide fusion technique with a detection limit of 0.01%. All measurements were converted to alpha, beta and gamma dose rates according to the conversion factors of Aitken (1985, 1998). Water content was directly measured and used to generate an estimate and uncertainty for pore water content since the time of sample deposition; estimates ranged from 14.7 ± 5.0% to 18.3 ± 5.0%. The cosmic-ray contribution to the dose rate was calculated from the burial depth, longitude, latitude, and elevation of the sample location following Prescott and Hutton (1994). Data were analyzed using the ANALYST program of Duller (1999).

In fluvial deposits, it is common for some sand grains to experience incomplete bleaching prior to deposition (Rittenour, 2008). This may occur for a number of reasons, including: attenuation of light though the water column (Berger, 1990), enhancement of light attenuation by increased suspended sediment concentrations during floods (Berger and Luternauer, 1987), direct contributions of non-bleached sediment from the erosion of older deposits and river banks (Rittenour, 2008), and/or limited solar exposure due to rapid erosion and transport during high discharge events (Rittenour, 2008). Even in deposits containing sands that were fully bleached at deposition, it is possible that these were mixed subsequently with younger, intrusive grains (Galbraith and Roberts, 2012). A useful test as to whether a sample was fully bleached prior to burial can be detected by examining the distribution or over-dispersion (OD) among D_e values obtained from many individual aliquots from the sample. OD is the amount of scatter left after all sources of measurement uncertainty are taken into account (Galbraith et al., 1999). In addition, histograms showing variations in the frequency of D_e measurements within the full range of sample D_e values can provide visual information as to whether the distribution is symmetrical or has a younger or older tail. We used both techniques in assessing bleaching of the six samples dated and to select the age model used.

4. Results

4.1. Paleochannel sedimentology and stratigraphy

Paleochannels are filled with 1.0–5.0 m of either massive, gray clay or thin, horizontally bedded, interstratified sand and clay that grade upward to muck, peat, or loamy sediments (Fig. 3, A–F). Typically, fine-grained paleochannel fill abruptly overlies and is readily distinguishable from light gray, coarse to gravelly coarse sand. This sand is interpreted as channel bed sediment on the basis of 1) its stratigraphic position and geomorphic context; 2) its textural similarity to the bedload of modern rivers in the region; and 3) the presence of rounded gravels, which suggests abrasion during transport in a channel environment. In cases where bedload sands are gradationally overlain by interstratified lenses of sand and clay, channel bed sand was discriminated from overlying, sandy paleochannel fill on the basis of its lack of interstratified clay and organic material, lighter color (10YR 5/1-7/1), higher gravel content, and greater resistance to penetration with a manual tile probe.

A profile from the thalweg of the Uvalda mega-meander of the Oconee River represents the sedimentology and stratigraphic relationships typical of deposits associated with large paleomeanders in the study area (Figs. 3A and 4). The profile contains 220 cm of fine-grained, clastic sediments that consist predominantly of massive, gray clay and abruptly overlie gravelly, coarse, single-grained sand. Grain-size composition and mass LOI data from the Uvalda profile quantitatively illustrate the distinct textural characteristics of paleochannel bed sediments versus younger channel fills that were clearly evident in auger boring hand samples from paleochannels investigated by this study.

Gravelly coarse sand of the 250–220 cm depth interval contains 10–18% gravel and a < 2 mm fraction with 94–96% sand and not > 4–6% silt plus clay (Fig. 4). Gravels are subrounded to rounded and range from 2.0–9.0 mm in diameter (−1 to −3.2 φ), while the sand fraction consists almost entirely of the 0.25–2.0 mm size fraction (2 to −1 φ), with very little fine or very fine sand. The grain size composition, clast roundness of the > 2 mm fraction, and stratigraphic position of the gravelly coarse sand at the base of the Uvalda profile suggest it was deposited as bedload in a relatively high energy, active channel bed environment. Grain diameter statistics for representative samples from the gravelly coarse sand of the Uvalda profile and the channel bed material of the modern Oconee River are reported in Table 3. Data indicate that the two groups of deposits have similar particle size distributions. Although paleochannel sediments (D_{50} = 0.84 mm) are slightly coarser than those of the modern Oconee channel bed (D_{50} = 0.48 mm), samples from both settings consist predominantly of sand in the 0.25–2.0 mm size range (Table 3). The textural similarity between paleomeander sands and the bedload of the modern Oconee River provides further support for the interpretation that the gravelly coarse sand at the base of the Uvalda profile represents paleochannel bed sediments. Comparable bedload grain size compositions have been

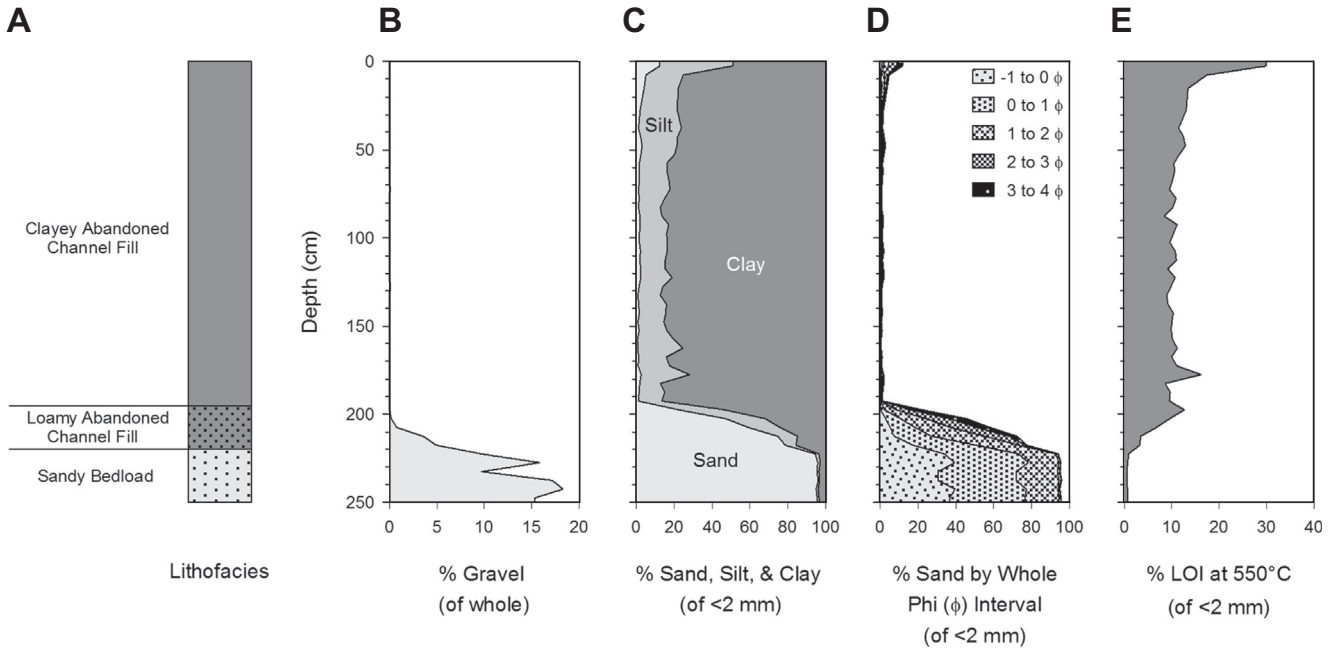

Fig. 4. Comparison of interpreted lithofacies (A) with grain size and loss-on-ignition data from a representative stratigraphic profile of the Uvalda mega-meander of the Oconee River. The profile was obtained from the thalweg of the paleochannel along cross-section A-A′ (see Fig. 3A, this paper, for location). Plots depict percent by weight of gravel (B); sand, silt, and clay (C); whole phi interval sand fractions (D); and loss-on-ignition (E) versus sample depth. Weight percentages are based on the sample whole for gravel and the < 2 mm fraction for other parameters. Samples were analyzed at approximately 5 cm depth increments for all variables. At this location, gravelly coarse sand extends to a depth of at least 310 cm beneath the ground surface.

observed for paleomeanders from alluvial settings elsewhere (Kozarski, 1983; Rotnicki, 1991; Wójcicki, 2006; Kasse et al., 2010).

The gravelly sand of the Uvalda profile is in abrupt contact with overlying loamy sediments that fine upward between 220 and 195 cm from a sandy loam (5.0% gravel, 79% sand) to a clay texture (0.0% gravel, 22% sand) and contain greater proportions of fine and very fine sand. Mass LOI is very low in the gravelly sand (< 1.0%) and increases abruptly from 3.0–13.0% in the loamy stratum from 220 to 195 cm. Loamy sediments above the contact with sand at 220 cm are interpreted as abandoned channel fill that accumulated immediately following meander cutoff. The fining of the sand fraction and consistent decrease in gravel and total sand content from 220 to 195 cm depth in loamy, basal abandoned channel fill probably represents a gradual decline in coarse sediment inputs, as cutoff bars formed at the entrance to the abandoned meander and progressively limited influx of bedload material when the channel was reoccupied during floods (Guccione et al., 2001).

Above a gradational contact with loamy sediments at 195 cm, the profile is composed entirely of massive to thinly laminated, gray clay that contains little sand (typically < 4%) and only negligible amounts of gravel. With the exception of higher values associated with a thin O horizon in the uppermost 10 cm of the profile, mass LOI in the gray clay is relatively consistent with depth, averaging ~11%. LOI in the Uvalda profile represents both organic matter content and structural water loss from clay minerals. The latter likely accounts for a substantial proportion of the observed mass LOI in the gray clay beneath a depth of 10 cm, because the unit is comprised mainly of clastic sediment, contains relatively modest amounts of organic material based on hand sample observations, and has very high clay content (Hoogsteen et al., 2015). These clayey sediments, which comprise the majority of channel fill, reflect sedimentation of clay- and silt-sized particles from suspension in an oxbow lake and later a meander scar environment.

Grain size data from the Uvalda profile support the stratigraphic position of the channel bed determined by field descriptions and demonstrate that textural properties evident in hand samples are reliable parameters for discriminating channel bed from basal channel fill sediments in the paleochannels examined in this study. Although variation exists in the sedimentology and stratigraphy among the mega-meander channel fills described herein (see Fig. 3), pronounced textural contrasts between paleochannel bed versus basal fill sediments similar to those of the Uvalda mega-meander were observed at four of the five other sites, including those along the Ogeechee, Congaree, Pee Dee, and Neuse Rivers (Figs. 3B, C, E, and F). This lends confidence to the accuracy of the channel boundaries delineated for these paleomeanders.

The Mouzon mega-meander (Fig. 3D) contains a sandier basal fill that was more difficult to discriminate from bedload sediments.

Table 3
Grain diameter statistics with percentages by weight of gravel and clay for paleo and modern channel bed sediments from representative localities in the lower Oconee River valley, Georgia.

Site	Maximum and specific percentile grain diameters (D_x) of channel bed sediment in millimeters (phi units)						Percent by weight of sample whole	
	D_{max}	D_{90}	D_{84}	D_{50}	D_{16}	D_{10}	Gravel (> 2 mm)	Clay (< 0.002 mm)
Uvalda Mega-meander	9.00 (−3.17)	1.97 (−0.98)	1.66 (−0.73)	0.84 (0.26)	0.39 (1.34)	0.31 (1.69)	9.72	3.34
Oconee River at Moses Point Bar, near Uvalda, Georgia	6.00 (−2.58)	1.23 (−0.30)	0.96 (0.06)	0.48 (1.05)	0.31 (1.71)	0.28 (1.86)	4.60	0.27

Rotnicki and Borówka (1985) note that channel fill may be hard to differentiate from active channel deposits when fill consists of fine-grained sands deposited in the paleochannel during reoccupation by post-abandonment floods. Although the channel boundaries delineated for the Mouzon mega-meander represent the most reasonable interpretation based on available data, the possibility exists that the uppermost part of the bedload sediment shown for this paleochannel (see 40–120 m cross-sectional distance interval, Fig. 3D) may consist of sandy, post-abandonment channel fill. Therefore, we caution that the cross-sectional area and resulting paleodischarge reported for this mega-meander (discussed in Section 4.4) should be regarded as conservative (or possibly under-) estimates.

In sand-bed streams, the channel bed may be scoured at high discharges then filled to the pre-flood level during the falling stage (Leopold et al., 1964). The upper boundary of bedload sediment depicted for each mega-meander in Fig. 3A–F is assumed to define the position of the paleochannel bed during bankfull flow. This interpretation follows Rotnicki's (1991) definition of the bankfull channel bed for alluvial paleomeanders (p. 453 and Fig. 20.9) and is consistent with the observation that scour is minimal in pool sections of sand-bed channels at flows equivalent to or less than the bankfull discharge (Andrews, 1979). Nevertheless, we cannot rule out modest scouring of paleochannel beds relative to their interpreted positions during bankfull discharge events. If such scouring occurred, the cross-sectional areas and paleodischarges reported in Section 4.4 would represent slight underestimates.

For all mega-meanders, paleochannel fill is bounded by sand associated with older fluvial deposits on the outsides of paleomeander bends. On the insides of bends, lateral accretion sediments overlain by finer-grained vertical accretion deposits typically less than 1 m thick bound channel fill. Upper lateral accretion sands of mega-meander point bars are usually finer than the coarse or gravelly coarse sand characteristic of lower parts of the channel bed, and this textural relationship is typical of such deposits (Rotnicki and Borówka, 1985). Nonetheless, mega-meander upper point bar sediments mainly consist of single-grained medium sand that can be clearly differentiated in hand samples from finer-grained overlying channel fill and overbank vertical accretion deposits. Because vertical accretion facies lacked evidence of buried ground surfaces or lithologic discontinuities indicative of continued sedimentation following channel abandonment, bankfull stage for all mega-meanders was defined as coinciding with the top of vertical accretion (i.e., the ground surface) on the crest of the point bar immediately adjacent to the paleochannel (Fig. 3A–F). However, we recognize the possibility that this placement may represent a slight overestimate of bankfull stage in instances where rates of pedogenesis equaled or exceeded overbank sedimentation rates following meander abandonment.

4.2. Paleochannel slopes

Because the slope of a paleochannel is not necessarily equivalent to that of its modern river counterpart (Rotnicki, 1991), paleochannel slope was field-surveyed at the Oconee, Ogeechee, and Neuse mega-meander sites, and field-measured estimates were used to evaluate the validity of slopes derived from valley gradients (Table 4). Paleochannel slopes based on the entire set of channel bed elevations per cross-section vary by a factor of 2.5, from 0.00016 (Ogeechee River, Cooperville FP-2 mega-meander) to 0.00041 (Oconee River Uvalda mega-meander).

To evaluate how different geomorphic components of the channel bed influenced variability in slope estimates, slopes were also calculated using the tops of fluvial bars, the thalweg, the predominant channel bed surface, and the lowest 20% of bed elevations per cross-section. For a given paleochannel, slope estimates from individual channel bed geomorphic components vary by as little as 0.00010 (a factor of 1.5), between the gradients of the predominant bed surface (0.00020) and mid-channel bars (0.00030) of the Neuse River Moccassin Creek mega-meander, to as much as 0.00068 (a factor of 3.8) between the gradient of mid-channel bars (0.00024) and the gradient of the thalweg (0.00092) of the Oconee River Uvalda mega-meander. However, no single geomorphic element of the channel bed results in consistent maximum or minimum slope values.

To account for uncertainty in mega-meander slope estimates resulting from variability in channel bed topography, minimum and maximum estimates based on the predominant channel bed surface and the lowest 20% of the channel bed were used in paleodischarge calculations. Slopes derived from the predominant bed surface (0.00020–0.00061) exclude elements of the channel bed that may be subject to extreme variability at the reach or cross-section scale (e.g., sand bars, thalweg scour holes) that are not representative of the overall channel gradient. Slope estimates based on the lowest 20% of channel elevations (0.00020–0.00078) are intended to provide an estimate of gradient derived from the lowest part of the channel bed, while simultaneously dampening the influence of localized variability in thalweg elevations. This estimate serves as the maximum gradient at two of the three sites where mega-meanders were field-surveyed (Table 4).

In all cases where mega-meander channel slopes were field-measured, the longitudinal valley gradient of the Qp3 geomorphic surface and the sinuosity-corrected valley gradient are either entirely bracketed by or are within 20% of minimum and maximum slope estimates based on the predominant channel bed surface and lowest 20% of the channel bed, suggesting that reliable estimates of paleochannel slope can be derived from valley gradients (Table 4). Therefore, for mega-meanders where field-measured slopes are unavailable (Congaree, Black, and Pee Dee River sites), maximum slope estimates (0.00028–0.00068) are based on the gradient of the Qp3 surface, while sinuosity-corrected gradients (0.00016–0.00040) serve as minimum slope estimates (Table 4). For all sites, a best estimate of paleochannel slope, obtained by averaging the minimum and maximum slope estimates, was used along with minimum and maximum values in paleodischarge calculations.

4.3. Paleochannel ages

Tables 5 and 6 respectively report radiocarbon and OSL age estimates for mega-meanders, and Fig. 5 provides a graphical depiction of age estimates and their associated uncertainties. Three of the four previously undated paleochannels (Oconee, Congaree, and Neuse River sites) returned calibrated radiocarbon ages that range from 11,815–16,917 cal yr BP, if the full breadth of the 2-sigma error is considered. These estimates are in good agreement with previously published radiocarbon and OSL dates of 13.3–13.8 ka for the Damon mega-meander of the Pee Dee River (Leigh et al., 2004; Fig. 3E, this paper) and dates reported from other sites in North Carolina and Georgia that indicate southeastern Coastal Plain rivers exhibited mega-meandering planforms during the terminal Pleistocene (Leigh, 2006, 2008). In addition, the 12,118–12,521 cal yr BP radiocarbon age obtained from basal channel fill of the Uvalda mega-meander is consistent with a 17,648–17,966 cal yr BP date from a well-preserved pine log collected in bedload sediments at 430–450 cm depth beneath a braided terrace correlative to the Qp2 alloformation at the Oconee River site (Table 5). These braided channel deposits are cross-cut by the Uvalda mega-meander (Fig. 3A) and immediately predate mega-meander alluvium in the lower Oconee valley (Suther, 2013, p. 45–51).

A terminal Pleistocene age is also indicated for the Cooperville FP-2 mega-meander of the Ogeechee River, based on a fresh looking seed obtained from a depth of 195–200 cm, at the base of mucky channel fill immediately atop channel bed sands, that yielded a calibrated date of 13,800–14,087 cal yr BP (Table 5, Fig. 3B). Although this estimate is considerably older than an 8320–8770 cal yr BP date reported by Leigh and Feeney (1995) from a fragment of unidentified wood obtained from a higher stratigraphic position elsewhere in the paleochannel, we

Table 4
Slope estimates derived from paleochannel geomorphic components and river valley gradients.

Site	Channel bed	Bar tops[a]	Thalweg	Predominant bed surface[b]	Lowest 20% of bed[c]	Paleochannel ground surface[d]	Valley gradient[e]	Sinuosity-corrected valley gradient[f]
Uvalda, Oconee R.	0.00041	0.00024	0.00092	**0.00028**	**0.00078**	0.00044	0.00039	0.00023
Cooperville FP-2, Ogeechee R.	0.00016	+	0.00029	**0.00061**	**0.00020**	0.00012	0.00038	0.00022
Running Creek, Congaree R.	–	–	–	–	–	–	**0.00068**	**0.00040**
Mouzon, Black R.	–	–	–	–	–	0.00023	**0.00030**	**0.00018**
Damon, Pee Dee R.	–	–	–	–	–	0.00016	**0.00028**	**0.00016**
Moccasin Creek, Neuse R.	0.00028	0.00030	0.00027	**0.00020**	**0.00026**	0.00043	0.00041	0.00024

[a] Tops of mid-channel bars. Plus sign for the Cooperville FP-2 site indicates the slope is inverted. This results from a pronounced mid-channel bar that is present at the middle and downstream cross-sections but absent at the upstream cross-section. For all columns, – = no data.
[b] The prevailing channel bed surface. Excludes the thalweg and tops of pronouced mid-channel bars. Bold values in this and the Lowest 20% of Bed Elevations column represent minimum or maximum slope estimates used in paleodischarge calculations for sites where slope was field-surveyed.
[c] The lowest 20% of bed elevations per paleochannel cross-section.
[d] Determined by field survey (Oconee, Ogeechee, and Neuse R. sites) or derived from LIDAR elevation data with a horizontal resolution of either 2 m (Pee Dee R. site) or 3 m (Congaree and Black R. sites).
[e] Longitudinal valley gradient of the geomorphic surface of the Qp3 alloformation. Bold values represent maximum slope estimates used in paleodischarge calculations for the Congaree, Black, and Pee Dee River sites.
[f] The slope that results if a sinuosity of 1.7, assumed to be representative of mega-meanders in the study area, is superimposed on the valley gradient. Bold values represent minimum slope estimates used in paleodischarge calculations for the Congaree, Black, and Pee Dee River sites.

believe that it provides a better estimate for the timing of meander abandonment than the early Holocene age, based on the quality of the dated material and its position at the very base of the paleochannel fill.

In contrast to the terminal Pleistocene dates discussed above, a middle Holocene calibrated radiocarbon age of 5147–5447 cal yr BP was obtained from a seed situated approximately 90 cm above channel bed sand in the thalweg of the Mouzon mega-meander of the Black River (Table 5, Fig. 3D). This age may be reasonable, given that mega-meanders dating to the early- to middle Holocene have been reported along the Ogeechee (Leigh and Feeney, 1995) and Canoochee (Leigh, 2006) Rivers in Georgia. However, it is likely that this date underestimates the time elapsed since meander abandonment, considering its relatively high position within the paleochannel fill at the thalweg location (Fig. 3D), and we therefore regard it with caution.

In this study, we dated six samples by OSL that were collected from scroll bars that respectively functioned as the active mega-meander point bar at each site shortly prior to the time of channel abandonment. OD values for the six samples ranged from 3.7 ± 0.2% (Cooperville FP-2) to 12.6 ± 0.7% (Uvalda, see Table 6). Taken at face value, these data suggest that the samples may not contain a mix of sand populations of very different age and do not contain grains that experienced vastly different levels of bleaching prior to burial. However, aliquot D_e frequency histograms show that the four Ogeechee, Congaree, and Black River samples have D_e distributions that are skewed towards higher doses that would increase the apparent ages of these samples (Fig. 6B–E).

Additionally, in a review paper, Duller (2008) emphasizes the relationship between aliquot size and the age obtained, and indicates that large aliquots (large = ca. 8 mm, medium = ca. 4.5 mm, small = ca. 2 mm; Fig. 2 in Duller, 2008) can mask partial bleaching in fluvial sands

Table 5
Radiocarbon dates and supporting data.

River and site	Lab no.	Sample depth (cm)	Height above bedload (cm)	Material dated	$\delta^{13}C$ corrected age ± 1 sigma (^{14}C yr BP)	Median probability (cal yr BP)[a]	2-σ calibrated range (cal yr BP)
Oconee River							
Uvalda Mega-meander	UGAMS 9553	198–203	2.5	Seeds	10,430 ± 30	12,308	12,118-12,521
Uvalda braided terrace	UGAMS 9719	430–450	–[b]	Pine log	14,620 ± 35	17,810	17,648-17,966
Ogeechee River							
Cooperville FP-2 Mega-meander	Beta-66163[c]	135	5	Wood	7700 ± 100	8500	8320–8770
Cooperville FP-2 Mega-meander	UGAMS 11794	195–200	2.5	Seed	12,090 ± 30	13,949	13,800–14,087
Congaree River							
Running Creek Mega-meander	UGAMS 11795	361	29	Seed pod	10,230 ± 30	11,962	11,815–12,106
Black River							
Mouzon Mega-meander	UGAMS 10374	165–170	90	Seed	4600 ± 25	5320	5147–5447
Pee Dee River							
Damon Mega-meander	UGA-10297[d]	260–275	–[e]	Acorn	11,470 ± 50	13,320	13,200–13,440
Neuse River							
Moccasin Creek Mega-meander	UGAMS 13645	225–235	5	Seeds	13,790 ± 40	16,678	16,450–16,917

[a] All dates were calibrated using the CALIB 7.1 radiocarbon calibration program (Stuiver et al., 2016) and the IntCal13 calibration curve.
[b] Sample obtained from within braided channel bedload (gravelly sand) at a position 339–359 cm beneath the top of bedload sediments.
[c] Previously reported in Leigh and Feeney (1995).
[d] Previously reported in Leigh et al. (2004).
[e] Sample obtained from the base of 2.7 m of peaty and clayey channel fill, immediately above gravelly sand (Leigh et al., 2004).

Table 6
Optically-stimulated luminescence (OSL) ages on quartz grains from mega-meander scroll bar sediments.

UGA sample ID	Sample depth (cm)	Number of aliquots	Grain size (μm)	CAM D_e (Gy)	MAM D_e (Gy)	Over-dispersion (%)	U (ppm)	Th (ppm)	K (%)	Water content (% by wt.)	Cosmic dose rate (Gy/ka)	Total dose rate (Gy/ka)	CAM age (ka)[a] ± 1 sigma	MAM age (ka)[b] ± 1 sigma
Oconee River - Uvalda														
11OSL-789	205–237	24 (22)	125–250	20.84 ± 0.58	15.98 ± 0.52	12.57 ± 0.72	1.41 ± 0.26	3.83 ± 0.92	0.70 ± 0.10	14.7 ± 5.0	0.144 ± 0.011	1.17 ± 0.13	17.9 ± 2.0	**13.7 ± 1.6**
Ogeechee River - Cooperville FP-2														
12OSL-810	178–210	24 (24)	125–180	13.55 ± 0.14	13.25 ± 0.14	3.72 ± 0.17	0.79 ± 0.24	4.00 ± 0.84	0.20 ± 0.10	18.3 ± 5.0	0.146 ± 0.011	0.65 ± 0.10	20.8 ± 3.3	**20.4 ± 3.3**
Congaree River - Running Creek														
13OSL-875	147–177	24 (16)	125–180	52.19 ± 0.97	48.46 ± 3.78	5.34 ± 0.41	3.30 ± 0.70	11.76 ± 2.42	1.70 ± 0.10	14.9 ± 5.0	0.159 ± 0.012	2.78 ± 0.27	18.8 ± 1.8	**17.4 ± 2.2**
Black River - Mouzon														
13OSL-909	150–181	24 (24)	125–250	13.36 ± 0.29	11.97 ± 0.35	9.35 ± 0.46	1.49 ± 0.18	2.83 ± 0.66	0.20 ± 0.10	16.5 ± 5.0	0.158 ± 0.012	0.72 ± 0.10	18.6 ± 2.6	**16.7 ± 2.4**
12OSL-808	210–242	27 (27)	125–250	10.05 ± 0.23	8.88 ± 0.24	8.68 ± 0.38	0.80 ± 0.09	1.16 ± 0.35	0.20 ± 0.10	17.1 ± 5.0	0.143 ± 0.011	0.49 ± 0.09	20.4 ± 3.6	**18.0 ± 3.2**
Pee Dee River - Damon														
DL-6[c]	120–150	NR[d]	NR	19.9 ± 2.7	NR	NR	1.0 ± 0.3	2.2 ± 0.9	1.19 ± 0.10	15.0 ± 5.0	0.150 ± 0.030	1.4 ± 0.1	13.8 ± 1.1	**NR**
Neuse River - Moccasin Creek														
13OSL-876	175–205	24 (18)	125–250	42.17 ± 1.28	36.50 ± 2.17	9.48 ± 0.63	1.37 ± 0.16	2.32 ± 0.60	1.70 ± 0.10	15.9 ± 5.0	0.152 ± 0.011	1.85 ± 0.15	22.7 ± 2.0	**19.7 ± 2.0**

[a] Calculated using the Central Age Model (CAM) of Galbraith et al. (1999).
[b] Calculated using the Minimum Age Model (MAM) of Galbraith et al. (1999). Bold ages signify that the MAM was selected as the appropriate age model for the fluvial sands dated (see Section 4.3).
[c] Previously reported in Leigh et al. (2004).
[d] NR = not reported.

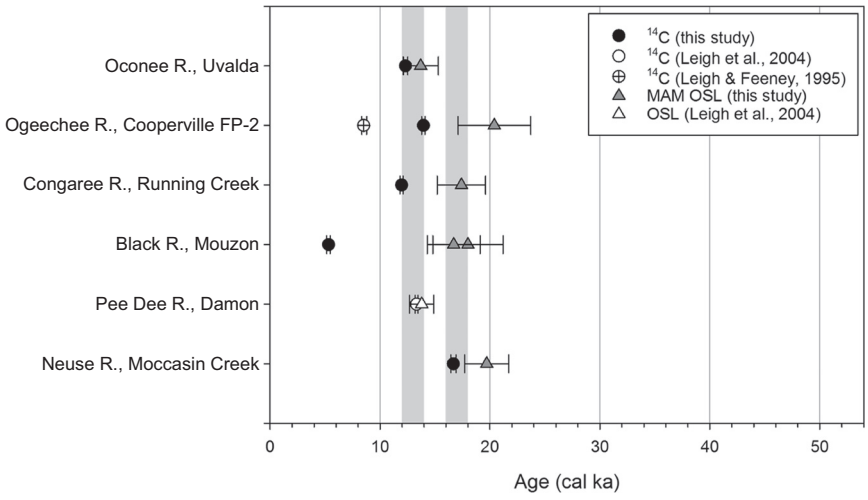

Fig. 5. Plot of radiocarbon and optically-stimulated luminescence (OSL) dates for mega-meanders. Previously published dates for the Cooperville FP-2 mega-meander of the Ogeechee River (Leigh and Feeney, 1995) and the Damon mega-meander of the Pee Dee River (Leigh et al., 2004) are also shown. Error bars represent one (OSL) and two (radiocarbon) standard deviation(s) of the age estimates. The light gray field represents the flow transition period from braided to meandering channels in the southeastern Atlantic Coastal Plain described by Leigh (2006) as having occurred between 16,000 and 14,000 calendar years before present. The dark gray field indicates the 18–12 ka interval, which encompasses both radiocarbon dates obtained from basal channel fill and the Minimum Age Model (MAM) OSL ages obtained by this study, if uncertainties are considered. The 18–12 ka interval is generally coincident with ages in the 16–11 ka range obtained from other large, scrolled paleomeanders elsewhere in the region (Leigh, 2008).

and produce age overestimates because of the increasing contribution of non-bleached grains to the total signal measured. An example of this effect is provided by Rittenour, who compared single grain minimum age model results with 5 mm aliquot ages to determine if the 5 mm aliquot size obscured inhomogeneous bleaching in three young fluvial samples from western Nebraska (See Fig. 1 of Rittenour, 2008). She found that the 5 mm ages were respectively 1.25, 0.85, and 0.77 kyr older than their single grain equivalents and concluded that averaging of thousands of grains in the aliquots had masked partial bleaching, producing overestimates of sediment burial age. Working with older fluvial samples, Srivastava et al. (2006) compared minimum ages for 9.6 mm and 4 mm aliquots of 120–150 μm quartz from the Homeb silts in the Kuiseb River valley of Namibia with single grain minimum ages. Six of the eight 9.6 mm minimum ages, which ranged from 9.8 ± 1.2 to 20.4 ± 3.3 ka, were older than the single grain equivalents by an average 2.77 kyr. They regarded the single grain ages to be more accurate, given the likelihood of partial bleaching in the dated sediments indicated by both their own bleaching studies and prior findings by Bourke et al. (2003).

Because our OSL ages were obtained on large (9.6 mm) aliquots, and because four of the six D_e frequency histograms are skewed towards higher D_e values (Fig. 6), both of which might lead to older than actual ages, we selected the Minimum Age Model (MAM) of Galbraith et al. (1999) as being more appropriate than the Central Age Model (CAM) for the fluvial sands dated. D_e determinations and resulting age estimates of both models are provided in Table 6, along with supporting data. The six MAM OSL ages obtained for lateral accretion and bedload sands beneath mega-meander point bars ranged from 13.7 ± 1.6 to 20.4 ± 3.3 ka (Table 6), and all are consistent with radiocarbon ages obtained from the earliest deposits of abandoned channel fill at the

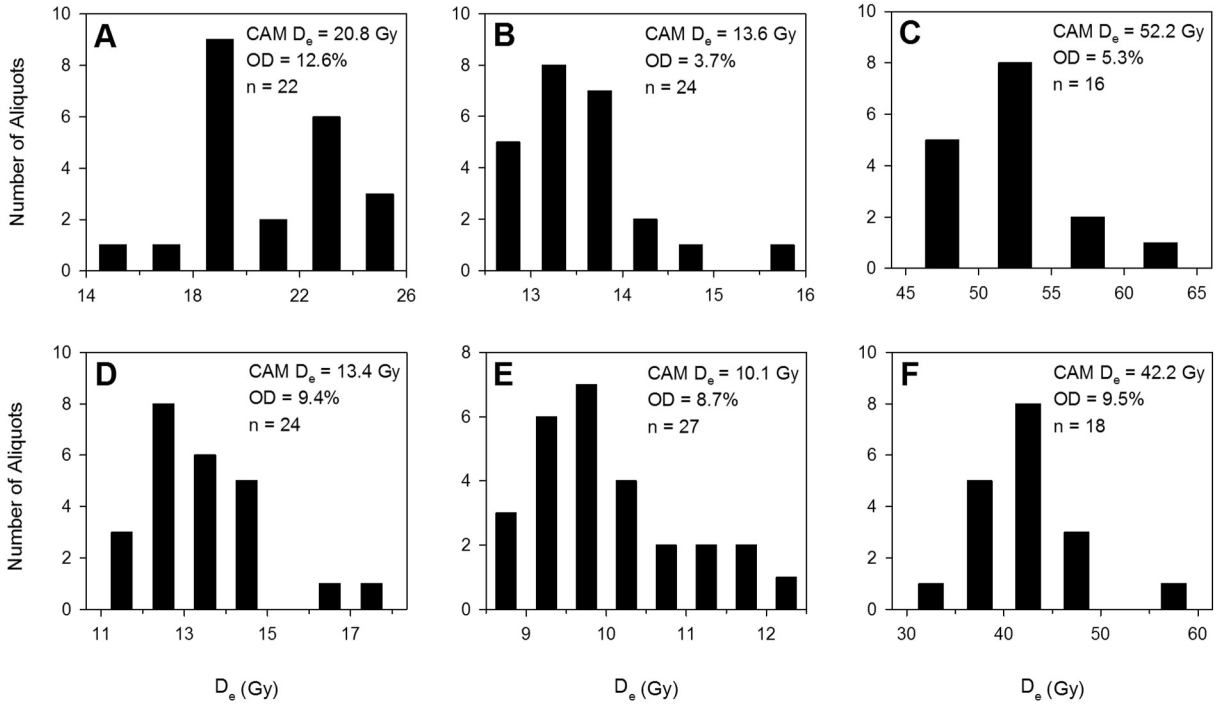

Fig. 6. Frequency distributions of equivalent dose (D_e) measurements obtained from 9.6 mm diameter aliquots of dated scroll bar sediments from the (a) Uvalda mega-meander, Oconee River (11OSL-789); (b) Cooperville FP-2 mega-meander, Ogeechee River (12OSL-810); (c) Running Creek mega-meander, Congaree River (13OSL-875); (d and e) Mouzon mega-meander, Black River (respectively 13OSL-909 and 12OSL-808); and (f) Moccasin Creek mega-meander, Neuse River (13OSL-876).

respective sites (Fig. 5). However, even when uncertainties are considered, for some mega-meanders the difference between the scroll bar OSL and channel fill radiocarbon dates is greater than anticipated for two sets of deposits that should be comparatively close in age. Therefore, we recognize the possibility that MAM OSL dates may be older than the actual ages of the sediments dated at some sites, particularly in the cases of the Ogeechee and Congaree River paleochannels. Evaluation of this possibility, potential explanations that may account for older OSL ages, and implications of paleochannel age estimates for refining our knowledge of the timing of large, scrolled paleomeanders in the southeastern Atlantic Coastal Plain are provided in Section 5.1.

4.4. Paleodischarge estimates

Paleodischarge estimates by the slope-area method indicate that bankfull discharges of mega-meanders were at least twice those of modern channels but within the range of two- to five-year recurrence interval flood magnitudes on present-day Atlantic Coastal Plain rivers (Tables 7, 8, and 9; Fig. 7). Larger than modern mega-meander bankfull discharge estimates are consistent with results of previous studies, which have inferred paleobankfull flows 1.3 to 4.2 times greater than modern values using equations that retrodict discharge based on paleochannel width, radius of curvature, and meander wavelength (Leigh and Feeney, 1995; Leigh, 2006).

To enable direct comparisons between paleo and modern discharge, mega-meander bankfull discharge estimates were compared to bankfull flows for modern rivers near paleochannel study sites. Modern discharge estimates were determined using the slope-area method and relied on field-surveyed channel cross-sections collected by the authors (Oconee River) or obtained from the Georgia and South Carolina offices of the USGS South Atlantic Water Science Center (Ogeechee, Black, and Pee Dee Rivers), the South Carolina Department of Transportation (Congaree River), and the North Carolina Floodplain Mapping Program (Neuse River). Modern channels at the cross-section locations have drainage areas that are either equivalent to or within 10% of those of their counterpart mega-meander sites for all rivers except the Neuse, where the modern cross-section has a drainage area about 17% smaller than that of the Moccasin Creek mega-meander. Techniques used for estimating channel slope and roughness for the cross-sections are reported in Table 8. Slope-area discharge estimates for modern channels were validated using bankfull discharge values determined from stage-discharge relations at nearby USGS gaging stations (Table 8), and channel cross-sections were located in the immediate vicinity of USGS gages for three of the six sites (Ogeechee, Black, and Pee Dee Rivers). Among rivers investigated in our study, the modern bankfull discharge has a return interval of 1.01 to 1.14 years in the annual series and, at most, half the magnitude of the two-year flood in the vicinity of mega-meander field sites (Table 8).

Best estimates by slope-area method indicate that mega-meanders conveyed at least twice the bankfull discharge of modern channels on the majority of rivers in the study area. Ratios of paleo to modern bankfull discharge by slope-area range from 1.6 to 4.1, while the average of ratios from all six rivers is 2.7 (Table 8). Slope-area estimates for modern channel cross-sections are within approximately 0.9 to 1.1 times the bankfull discharge at the closest USGS gaging station for four of the six sites (Oconee, Congaree, Pee Dee, and Neuse), indicating good agreement between estimated and gaged values for these rivers (Table 8). For modern channels of the Ogeechee and Black Rivers, the slope-area method respectively overestimates gaged bankfull discharge by a factor of 1.6 (115 vs. 73 m^3/s and 62 vs. 39 m^3/s), but paleodischarge is nonetheless respectively 1.6 and 2.1 times larger than slope-area estimates of the modern bankfull flow at these locations. Despite differences in estimated versus gaged modern discharge on the Ogeechee and Black Rivers, across the entire dataset, ratios of paleo to modern discharge using the gaged bankfull flow size are similar to ratios based on slope-area estimates, yielding values ranging from 1.8 to

Table 7
Bankfull discharge estimates and supporting data for mega-meander paleochannels.

Site and river	Cross-sectional parameters[a]				Slope			Manning's *n*			Velocity (m/s)			$PaleoQ_{BKF}$ (m^3/s) by slope-area[b]		
	W/D	CSA (m^2)	WP (m)	R	Min	Best estimate	Max	Min	Best estimate	Max	Min	Best estimate	Max	Min	Best estimate	Max
Uvalda, Oconee	121.2	649.6	261.4	2.5	0.00028	0.00053	0.00078	0.030	0.038	0.045	0.69	1.11	1.71	445	**723**	1110
Cooperville FP-2, Ogeechee	95.7	251.1	150.4	1.7	0.00020	0.00041	0.00061	0.030	0.038	0.045	0.45	0.75	1.16	112	**188**	292
Running Creek, Congaree	144.3	1533.3	462.9	3.3	0.00040	0.00054	0.00068	0.030	0.038	0.045	0.99	1.36	1.93	1514	**2084**	2962
Mouzon, Black	55.2	210.0	114.6	1.8	0.00018	0.00024	0.00030	0.030	0.038	0.045	0.44	0.61	0.86	93	**128**	182
Damon, Pee Dee	166.3	2180.9	541.4	4.0	0.00016	0.00022	0.00028	0.030	0.038	0.045	0.72	0.99	1.41	1575	**2167**	3080
Moccasin Creek, Neuse	166.7	639.5	304.1	2.1	0.00024	0.00033	0.00041	0.030	0.038	0.045	0.57	0.78	1.11	362	**498**	709
	Average = 124.9			Average = 2.6												

[a] See Table 2 for definitions of W/D, CSA, WP, and R.
[b] Paleobankfull discharge calculated by the slope-area method. Bold values indicate best estimates.

Table 8
Bankfull discharge estimates for modern rivers near mega-meander study sites, with ratios of paleo to modern discharge provided for comparison.

River and site[a]	Drainage area (km^2)	Modern river site/mega-meander drainage area	Cross-sectional parameters[b]				Slope[c]	Manning's n[d]		
			W/D	CSA (m^2)	WP (m)	R		Min	Max	Best estimate
Oconee at Moses Point Bar, near Uvalda, GA	13,737	1.00	77.3	383.5	165.2	2.3	0.00032	0.030	0.040	0.035
Ogeechee at GA Hwy 24, near Oliver, GA	6138	1.10	25.1	148.7	61.2	2.4	0.00022	0.030	0.040	0.035
Congaree at US-601, near Fort Motte, SC	22,062	1.00	23.6	610.0	136.6	4.5	0.00021	0.030	0.040	0.035
Black at US-52, Kingstree, SC	3243	1.07	17.4	172.2	57.0	3.0	0.00004	0.030	0.040	0.035
Pee Dee at US-76/301, near Pee Dee, SC	22,870	1.10	15.7	557.3	107.1	5.2	0.00012	0.030	0.040	0.035
Neuse near Brodgen, NC	4095	0.83	22.8	163.9	65.5	2.5	0.00031	0.030	0.040	0.035
			Average = 30.3			Average = 3.3				

River and site[a]	Velocity (m/s)			Q_{BKF} (m^3/s) by slope-area[e]			Q_{BKF} determined from nearest gage			Q_2 by regional curve[i] (m^3/s)	PaleoQ$_{BKF}$/ modern slope-area Q_{BKF}[j]	PaleoQ$_{BKF}$/ modern gaged Q_{BKF}[j]
	Min	Max	Best estimate	Min	Max	Best estimate	Q_{BKF}[f]	Q_{BKF} recurrence interval (yr)[g]	USGS gaging station[h]			
Oconee at Moses Point Bar, near Uvalda, GA	0.78	1.04	0.89	298	398	**341**	**396**	1.14	Mt. Vernon, GA #02224500	864	**2.12**	**1.82**
Ogeechee at GA Hwy 24, near Oliver, GA	0.68	0.90	0.77	101	134	**115**	**73**	–	Oliver, GA #02202190	300	**1.64**	**2.60**
Congaree at US-601, near Fort Motte, SC	0.99	1.32	1.13	605	807	**691**	**787**	1.01	Gadsden, SC #02169625	1555	**3.02**	**2.65**
Black at US-52, Kingstree, SC	0.32	0.42	0.36	54	73	**62**	**39**	1.06	Kingstree, SC #02136000	154	**2.05**	**3.30**
Pee Dee at US-76/301, near Pee Dee, SC	0.83	1.11	0.95	462	616	**528**	**510**	1.05	Pee Dee, SC #02131000	1447	**4.10**	**4.25**
Neuse near Brodgen, NC	0.81	1.09	0.93	133	178	**153**	**145**	1.03	Smithfield, NC #02087570	354	**3.25**	**3.45**
											Average = **2.70**	**3.01**

[a] The Oconee River cross-section is shown in Fig. 8. Cross-sections for other rivers are depicted in Supplementary Figs. 1–5.
[b] See Table 2 for definitions of W/D, CSA, WP, and R.
[c] Channel slope was measured from field-surveyed cross-sections (Neuse River) or the best available elevation mapping (all other sites).
[d] Manning's n values were estimated by criteria specified in Arcement and Schneider (1989) and by visual comparison with the viewbook of Barnes (1967).
[e] Modern bankfull discharge estimated using the slope-area method and field-surveyed cross-sections.
[f] Bankfull discharge at each gaging station was determined using a stage-discharge relation developed from gage records. Gage height for bankfull discharge was verified using banktop elevations of field-surveyed channel cross-sections and floodplain elevations determined from the best available elevation data for each locality.
[g] The recurrence interval for the Congaree River near Gadsden is based on the bankfull discharge exceedance probability of 0.99 reported by Patterson et al. (1985). All other estimates were calculated from gage records using the Log Pearson Type III method. A return interval is not reported for the Ogeechee River near Oliver, GA because the period of record at gage #02202190 is too short to support flood frequency analysis. Bankfull discharge of the Ogeechee River near Eden, GA approximately 50 km downstream from Oliver has a return interval of 1.07 years (Table 2).
[h] For the Ogeechee, Black, and Pee Dee River sites, modern channel cross-sections are located in the immediate vicinity of the referenced gaging station, and the gage and cross-section have the same drainage area. For the other sites, the gage closest to the modern channel cross-section is shown. Drainage areas for the Oconee River near Mt. Vernon, GA, Congaree River near Gadsden SC, and Neuse River at Smithfield, NC stations are respectively 13,235, 21,471, and 3124 km^2.
[i] Values for the 2-year recurrence interval flood (Q_2) for the Oconee, Ogeechee, Black, and Neuse River cross-sections were calculated by weighting regional curve estimates with flow data from the nearest gaging station with ≥20 years of record, according to the methods described in Table 1. Because data required to calculate weighted discharge were not available for the Congaree and Pee Dee Rivers, unweighted regional curve estimates are reported for these sites.
[j] Ratios of paleo to modern bankfull discharge, as well as the slope-area best estimates and gaged values of modern discharge used to calculate the ratios, are given in bold. Discharge ratios are based on best estimates of paleobankfull discharge (see Table 7).

Table 9
USGS regional flood frequency curve estimates of the two-year recurrence interval discharge for modern rivers at mega-meander study sites.

Site and river	Q_2 (m^3/s) by regional flood frequency curves[a]			Weighted Q_2[a] (m^3/s)	PaleoQ_{BKF}/modern Q_2[b]
	Lower limit, 95% prediction interval	Mean	Upper limit, 95% prediction interval		
Uvalda, Oconee	416	799	1535	864	0.84
Cooperville FP-2, Ogeechee	152	292	561	303	0.62
Running Creek, Congaree	807	1555	3002	–	1.34
Mouzon, Black	86	166	320	150	0.85
Damon, Pee Dee	753	1450	2790	–	1.49
Moccasin Creek, Neuse	220	422	810	360	1.39
					Average = 1.09

[a] See Table 1 for methods used to calculate the regional flood frequency curve and weighted estimates of the modern 2-year recurrence interval flood (Q_2).
[b] Ratio of the paleobankfull to modern 2-year discharge. The mean Q_2 predicted by the regional flood frequency curve was used for the paleoQ_{BKF}/modern Q_2 ratio for the Congaree and Pee Dee sites, where weighted estimates of Q_2 were unavailable. The weighted estimate of Q_2 was used in all other cases.

4.3 and averaging 3.0 among all six sites (Table 8). These results provide further evidence that mega-meander discharge at the bankfull stage was at least roughly double that of modern values for rivers examined in this study.

Mega-meander bankfull flows were also evaluated against the two- through 25-year recurrence interval flood discharges for modern rivers adjacent to paleochannel field sites (Gotvald et al., 2009b). This comparison places paleobankfull flow within the context of modern flood magnitudes and is intended to illustrate where mega-meander bankfull discharge falls in comparison to familiar modern flood sizes along rivers. The two-, five-, 10-, and 25-year floods were selected for use because they represent standardized discharges within the modern fluvial system that are recognized by most workers and easily estimated for ungaged sites using established USGS regional regression curves (Gotvald et al., 2009b). These modern discharges are employed here strictly as a reference frame to support comparison of paleobankfull flows versus contemporary flood magnitudes and are not meant to imply a particular return interval for mega-meander bankfull discharge.

Best estimates of paleobankfull and modern flood discharges indicate mega-meander bankfull discharges were within the size range of two- to five-year flood magnitudes on the majority of evaluated rivers (Table 9, Fig. 7). Ratios of the paleobankfull to modern two-year recurrence interval discharge range from 0.6 (Cooperville FP-2 mega-meander, Ogeechee River) to 1.5 (Damon mega-meander, Pee Dee River), while the average of the ratios from all six mega-meanders is 1.1 (Table 9). Among study sites, paleochannels most likely to have conveyed bankfull flows that were larger than the modern two-year recurrence interval discharge include the Neuse, Pee Dee, and Congaree mega-meanders. The ratios of paleobankfull to modern two-year discharge for these mega-meanders range from 1.3 to 1.5. Considering the full breadth of uncertainty in both paleo and modern two-year discharge estimates (Fig. 7), mega-meander bankfull discharge may have been as low as the two-year flood size along these three rivers or possibly as high as a magnitude exceeding that of the 10-year flood, in the case of the Pee Dee and Congaree sites. However, best estimates suggest paleobankfull discharge for these rivers ranged from about 40% greater than the modern two-year flood size along the Neuse River to a magnitude equivalent to that of the five-year flood on the Pee Dee (Fig. 7).

5. Discussion

Mega-meander channel-forming discharges were at least twice as large as bankfull flow magnitudes on present-day Atlantic Coastal Plain rivers in the southeastern US. This finding is consistent with results from previous research, which relied on comparatively less precise estimates from regression equations that retrodict discharge based on planform meander dimensions (Leigh and Feeney, 1995; Leigh, 2006). The present study represents an improvement upon earlier work, in that the estimates here are based on principles of open-channel hydraulics and account for paleochannel cross-sectional dimensions and slope,

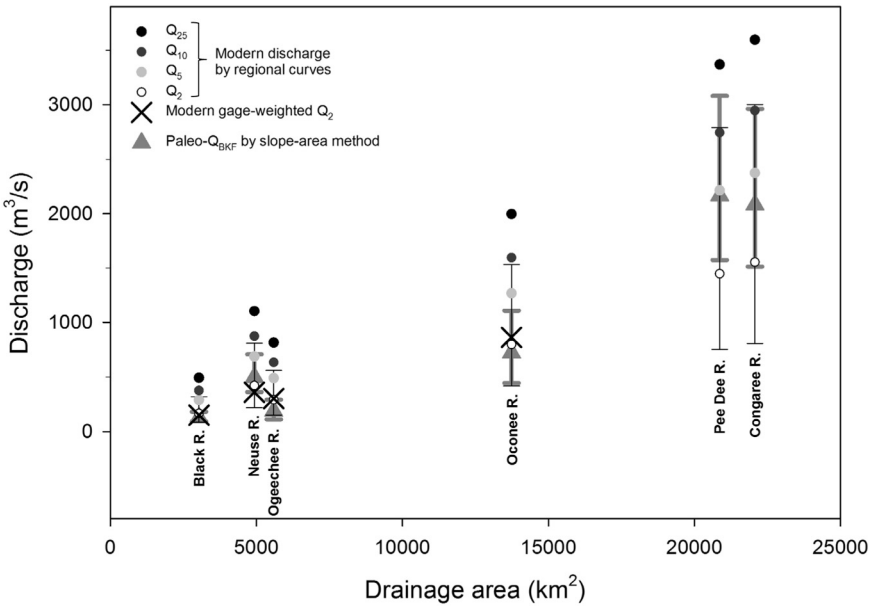

Fig. 7. Mega-meander bankfull discharge (Paleo-Q_{BKF}) and discharge of the two-, five-, 10-, and 25-year recurrence interval floods on modern rivers adjacent to mega-meander sites. Modern discharge was estimated at ungaged mega-meander sites using regional flood frequency regression curves (circles). For the two-year recurrence interval flood, weighted discharge is shown where available (X's). Weighted discharge improves the regional regression estimate by incorporating flood frequency data from the nearest gage. Error bars for mega-meander bankfull discharge represent minimum and maximum discharges based on minimum and maximum estimates of channel roughness and slope. For regional curve estimates, the lower and upper limits of the 95% prediction interval are shown for the two-year discharge (thin, black error bars). For five, 10-, and 25-year discharges, only the best estimate is shown.

which were previously unknown for these paleomeanders. The discussion that follows evaluates the timing of scrolled mega-meanders in the study area, possible paleoclimatic drivers of large bankfull flows, and relationships between paleochannel cross-sectional shape and discharge. The influence of historical impacts on paleo versus modern channel interpretations, the role of sedimentologic controls on mega-meander channel morphology, paleochannel response to late Quaternary sea-level change, and implications for paleodischarge estimation in comparable alluvial settings are also addressed.

5.1. Time of scrolled mega-meanders

For the four previously undated mega-meanders where we obtained new radiocarbon age estimates from the earliest deposits of abandoned channel fill (Oconee, Ogeechee, Congaree, and Neuse River sites), calibrated two-sigma ages range from 11.8–16.9 cal ka (Table 5). These dates are in good agreement with previously reported age estimates from other localities in the southeastern Coastal Plain (Leigh, 2006, 2008) that indicate rivers in the region had large meandering patterns during the terminal Pleistocene. The six MAM OSL ages obtained by this study from mega-meander point bar sands range from 13.7 ± 1.6 to 20.4 ± 3.3 ka (Table 6) and are consistent with radiocarbon ages obtained from channel fill at the respective sites (Fig. 5). In the case of the Uvalda mega-meander of the Oconee River, the radiocarbon and MAM OSL ages overlap, suggesting paleochannel abandonment at or shortly before 12.1–12.5 ka. The radiocarbon and MAM OSL ages for the Moccasin Creek mega-meander on the Neuse River are also close, being within 0.8 kyr if uncertainties are considered (16.5–16.9 ka versus 19.7 ± 2.0 ka), indicating paleochannel abandonment at or immediately prior to circa 17 ka.

However, even when uncertainties are considered, the MAM OSL ages for the Cooperville FP-2 (Ogeechee River) and the Running Creek (Congaree River) mega-meanders are respectively at least 3.0 kyr and 3.1 kyr older than their counterpart radiocarbon ages (13.8–14.1 ka vs. 20.4 ± 3.3 ka and 11.8–12.1 vs. 17.4 ± 2.2 ka). Although we expect the OSL ages to be older, the difference between the scroll bar OSL versus channel fill radiocarbon dates for these paleomeanders is greater than anticipated for two groups of deposits that should exhibit relatively close temporal correspondence. This age difference does not appear to be attributable to contamination of radiocarbon samples by younger organic matter or erroneous interpretation of the stratigraphic context of dated material. For all sites, radiocarbon samples consisted of unabraided, intact plant macrofossils (seeds) that were thoroughly cleaned prior to dating. Except for the case of the Black River mega-meander discussed above, dated materials were sampled from in-situ positions at the very base of paleochannel fill directly above gravelly channel bed sands. Thus, radiocarbon ages should correspond to the time immediately following meander abandonment, and we therefore regard them as excellent indicators of when the Oconee, Ogeechee, Congaree, and Neuse mega-meanders last functioned as active channels.

Discrepancies between radiocarbon and OSL ages for the Ogeechee and Congaree sites notwithstanding, scroll bar MAM age estimates show general correspondence to previously reported radiocarbon and OSL dates for correlative paleomeanders from other locations in the southeastern US. Leigh (2006, 2008) indicates that scrolled mega-meanders elsewhere in the region date to the 11–16 ka interval. Before this, from circa 16–30 ka, the Oconee-Altamaha, Pee Dee, and other southeastern rivers were characterized by braided channels and associated riverine eolian dunes (Leigh et al., 2004; Leigh, 2008). Notably, the Late Pleistocene radiocarbon and MAM OSL ages in Fig. 5 all fall within the time frame of 12–18 ka if uncertainties are considered, a period roughly subsequent to the late Wisconsin interval of braided channels (16–30 ka) and nearly coincident with the 11–16 ka interval of scrolled mega-meanders documented by previous studies (Leigh, 2006, 2008). In fact, if age uncertainties are considered, five of the seven OSL ages shown in Fig. 5 overlap the 14–16 ka flow-transition period described by Leigh (2006), when many rivers of the southeastern Atlantic Coastal Plain appear to have shifted from braided to large meandering patterns in response to climate-mediated changes in vegetative cover, sediment supply, runoff, and bank stability.

Despite the reasonable correspondence between our new age data and previous dating in the region, we suspect that some of the MAM OSL ages reported here may be erroneously older than the actual ages of the dated sediments. One source of error may be low-biased annual dose rate estimates, resulting from K depletion by weathering of scroll bar sediments following their burial. This is of particular concern for the three Ogeechee and Black River ages, which are based on extremely low K concentrations of 0.20 ± 0.10%, compared with values of 0.7–1.7% for the other three dated samples (Table 6). The low K values for the Ogeechee and Black River sediments reduced the dose rate estimates for these samples, and so increased their estimated ages. Ivester (1999) found that Coastal Plain-sourced fluvial sediments in Georgia have consistently lower K concentrations than sediments of Piedmont-sourced rivers, and Ivester and Leigh (2003) report a clear trend in K depletion with time in late Quaternary riverine eolian dunes sourced from the alluvium of Coastal Plain-draining rivers. Given their Coastal Plain source areas, the Ogeechee and Black River sediments probably had initally low K concentrations and may have been especially sensitive to percentage reductions below their K values at burial. If so, and K was further depleted from these sediments due to leaching by percolating ground water, then we may have underestimated the annual dose rate that produced the D_e values for the Ogeechee and Black River samples and thus overestimated their age.

In addition to the possibility of dose rate underestimation, we have shown previously that, despite low OD values, the sand grains in the dated samples were probably not all fully bleached at the time of deposition. This circumstance would yield older ages and was possibly exacerbated by our use of large aliquots (9.6 mm) in the dating process, which are known to produce older age estimates than small aliquots or single grains in cases of inhomogeneous bleaching.

In light of these considerations, we must entertain the distinct possibility that some of the MAM OSL ages reported here are overestimates. At many localities, including the Oconee, Congaree, Black, and Neuse River sites (Fig. 3), mega-meanders cross-cut braided river terraces correlative to the Qp2 alloformation (Fig. 2) and older deposits. Leigh (2008, p. 104) notes that the sandy scroll bars typical of terminal Pleistocene mega-meanders likely reflect reworking of sand and gravel sourced directly from lateral erosion by the large meanders into older, sandy braided channel sediments. Thus, it is possible that some scroll bar sands were eroded from nearby valley-flanking braided river sediments, then transported in conditions that precluded solar resetting (at night or in muddy water), and deposited and rapidly buried without exposure to sunlight. In such a scenario, rather than dating the most recent mega-meander point bars, scroll bar OSL dates would instead reflect at least some contribution from older, unbleached braided terrace sands. Given that the most recent phase of braiding in river valleys of the region dates to the late Wisconsin interval, circa 16–30 ka (Leigh, 2008), and that mega-meanders cross-cut braided river deposits in many locations, including at four of the six study sites, inherited age from unbleached, cannibalized braided terrace sands is a likely source of the discrepancy that exists between some of the MAM OSL ages and younger radiocarbon dates reported in this paper.

Another possibility that we cannot rule out is that mega-meandering patterns were established prior to 16–17 ka on some rivers in the region. However, this conclusion is not supported for the Oconee-Altamaha, Pee Dee, or Ogeechee River valleys, where a large set of radiocarbon and luminescence dates obtained from braided river sediments, eolian deposits, and large paleomeanders clearly indicate that the late Wisconsin interval of 16–30 ka was characterized by braided channels and associated riverine eolian dunes, while rivers in the terminal Pleistocene (11–16 ka) exhibited scrolled, mega-meandering

patterns (Ivester et al., 2001; Leigh et al., 2004; Leigh, 2006, 2007, 2008). On the Altamaha and Pee Dee, OSL dates for braided river and related eolian dune deposits were validated against radiocarbon ages from stratigraphically similar (Leigh et al., 2004) or bracketing (Ivester et al., 2001) positions and were obtained from sediments with a high likelihood of signal resetting (upper braid bar or eolian sand), lending high confidence to the timing of braiding established by previous studies for these rivers. The time of most recent braiding is also reasonably constrained for the lower Oconee River, a tributary to the Altamaha, where our 17,648–17,966 cal yr BP radiocarbon date (Section 4.3 of this paper, Table 5, Fig. 3A), along with two previously published 22.4 ± 4.2 and 27.9 ± 4.4 ka OSL ages (Leigh et al., 2004) obtained from a braided terrace into which the Uvalda mega-meander is cross-cut, indicate that the river was braided during the late Wisconsin stage up to circa 18–17 ka and did not shift to a large meandering pattern until after that time.

On the other hand, in the Congaree, Black, and Neuse River valleys, where correlative Late Pleistocene braided river deposits have not been numerically dated, one might wonder if mega-meandering planforms were established before 16–17 ka. The only site for which radiocarbon age data corroborate this interpretation is the Moccasin Creek mega-meander, where well-preserved seeds situated 5 cm above bedload sediments returned an age of 16,450–16,917 cal yr BP (Table 5). This date indicates that the Moccasin Creek paleochannel was abandoned shortly prior to 16.5–16.9 ka and, when considered along with laterally extensive scrollwork topography preserved on the interior of this paleomeander (Fig. 3F), implies that a sinuous, large meandering pattern was well-established on the Neuse by circa 17 ka. In fact, if uncertainties are considered, our scroll bar MAM OSL age of 19.7 ± 2.0 ka falls within 0.8 kyr of the 16.5–16.9 ka estimate based on the radiocarbon age, as noted above. Because the Mocassin Creek mega-meander appears to have last functioned as the active channel of the Neuse River around 17 ka, then it is possible that mega-meandering planforms were also established on the Congaree and Black Rivers at this time. From this viewpoint, the ages for the scroll bar sediments of paleomeanders along these rivers (17.4 ± 2.2, 16.7 ± 2.4, and 18.0 ± 3.2 ka) may actually be evidence of a slightly earlier transition from braided to meandering in the region than previously thought. However, a radiocarbon date of 11.8–12.1 ka obtained from a high quality seed pod in the basal fill of the Running Creek mega-meander argues against this possibility in the case of the Congaree River.

Taking into account the above considerations, among the new age data obtained by this study, we believe that the radiocarbon dates provide the best estimates of when mega-meanders last functioned as active channels. For the Oconee, Ogeechee, Congaree, and Neuse mega-meanders, this appears to have been during the terminal Pleistocene, at or shortly before 11.8–16.9 ka. MAM OSL and radiocarbon dates returned terminal Pleistocene and mid-Holocene ages for deposits associated with the Mouzon mega-meander of the Black River. However, this paleomeander remains to be more precisely dated, because the 5.1–5.5 ka radiocarbon age reported for the paleochannel was obtained from sediments that likely post-date meander cutoff. Subsequent field visits did not yield material suitable for dating from deeper positions within its channel fill.

5.2. Paleoclimatic drivers

Previous studies have relied on mega-meander paleodischarge estimates in conjunction with regional pollen and global paleoclimate proxy records to infer seasonally wetter conditions, greater runoff, and larger bankfull flows for the terminal Pleistocene versus late Holocene and modern time in the southeastern Atlantic Coastal Plain (Leigh, 2006, 2008). Our results support this interpretation. Although the specific paleoclimatic drivers that produced greater discharge during the terminal Pleistocene are not well known, the larger bankfull flows of this interval appear to reflect dynamic changes to precipitation delivery and runoff.

Leigh (2008) notes that around 16 ka vegetation cover represented in pollen sections of the southeastern Atlantic Coastal Plain began changing from the savanna-like jack pine-spruce forest of the late Wisconsin interval to a cool-mixed to temperate deciduous forest, reflecting a shift to warmer, more moist conditions that characterized study area paleoclimate during the terminal Pleistocene (Watts, 1980; Hussey, 1993; Webb et al., 2004; LaMoreaux et al., 2009). Such regional change occurred as conditions in the North Atlantic, which began cold circa 17–16 ka, warmed rapidly until the Younger Dryas cold excursion of 12.7–11.5 ka (Alley, 2000; Bard, 2002). Watts (1980) contends that the study area during this time was cooler and more moist than today based on the expansion of *Fagus* (beech) at the White Pond pollen site, on the inner Coastal Plain of South Carolina. Similar, contemporaneous increases in beech abundance have been documented in other pollen sections throughout the region (Frey, 1951; Hussey, 1993; LaMoreaux et al., 2009). Moist conditions within this timeframe are also indicated by terrestrially-derived *n*-alkane hydrogen isotope records from Jones and Singletary Lakes in eastern North Carolina (Lane et al., 2018), which suggest increased moisture availability and decreased evapotranspiration during the 15–13 ka interval. Watts (1980) argues the abundance of beech during the terminal Pleistocene indicates that greater water availability existed during the spring and summer growing season. Such increased spring and summer moisture may have been juxtaposed against a dry fall or winter, as implied by 15 ka riverine eolian dunes associated with the Damon mega-meander that suggest seasonal dryness occurred in the Pee Dee valley (Leigh et al., 2004; Fig. 3E, this paper). These dunes (and others like them affiliated with mega-meanders elsewhere in the region) were derived from sandy scroll bars and may have been active during a low-flow dry season, when fresh sands deposited during a preceding flood season were deflated from paleochannel point bars and floodplain sources. Leigh (2008) indicates that winters were cold and summers were mild in the study area from 16 to 11 ka, based on respective average January and July temperature estimates of −5.7 and 19.6 °C for the White Pond locality by Watts (1980), and comparable modern analog pollen-derived mean July temperature estimates of 20–23 °C by Viau et al. (2006) for central South Carolina during the 14–11 ka timeframe.

The regional temperature and moisture characteristics described above suggest that annual water balance and landscape conditions during the terminal Pleistocene may have contributed to the larger bankfull flows that mega-meanders conveyed. Greater discharge was likely facilitated by cool temperatures during this time, which would have resulted in lower than modern evapotranspiration rates and higher effective precipitation. Another possible cause of larger floods includes increased discharge associated with a snow melt runoff season (Leigh, 2008) or rain on snow, given that the cold winter temperatures of this interval would have allowed snowpack accumulation during the late winter and early spring. Dury (1965) cited rain on frozen ground as a possible driver for large paleomeanders and modern underfit channels similar to those found in the Southeast, and this mechanism may have also promoted higher discharge during this timeframe. French and Millar (2014) present a revised map that tentatively extends the southern limit of Last Glacial Maximum (LGM) discontinuous permafrost originally mapped by Péwé (1983) into the Blue Ridge Mountains and Appalachian Piedmont of the Carolinas and northeast Georgia. Unequivocal evidence for LGM permafrost in the form of sand-wedge casts and sediment-filled pots has been described 300 km to the north, in the mid-Atlantic Coastal Plain (French et al., 2009), but has not been documented within the study area. However, if at least seasonally frozen soils persisted through the terminal Pleistocene in the region, rain or snow melt on frozen ground may have increased runoff during a spring flood season.

Dynamic aspects of paleoclimate resulting in increased precipitation (at least on a seasonal basis) may have also favored greater bankfull discharge during the terminal Pleistocene. Frontal precipitation

produces seasonally higher runoff in winter and early spring in the region under the modern climate (see Section 2.2). Large temperature contrasts between high-latitude (Bard, 2002) and tropical (Lea et al., 2003) oceans at the end of the Pleistocene, along with a northward shift of the polar jet as the circumpolar vortex contracted in response to ablation of the Laurentide ice sheet (Rich et al., 2011), may have focused storm-track associated moisture on the southeastern US and promoted increased winter and springtime frontal precipitation relative to modern conditions. Indeed, such a moisture source would have provided not only greater seasonal precipitation, but its timing during the water year would have allowed for amplification of spring discharge via snowmelt runoff and possibly rain on snow or frozen ground, assuming these mechanisms operated in the study area. The large channel-forming discharge of mega-meanders could alternatively reflect increased seasonal runoff from tropical storms, given that sea surface temperatures in the tropical Atlantic were relatively high before and after the Younger Dryas (Lea et al., 2003). These weather systems have a distinct influence on the region's modern flood hydroclimatology (Gamble and Meentemeyer, 1997), and increased frequency and/or magnitude of landfalling tropical storms have been cited as a possible cause of more pronounced overbank flooding and larger than modern paleochannel dimensions in the region during the early Holocene (Goman and Leigh, 2004; Leigh and Feeney, 1995). However, if pronounced summertime precipitation was not firmly established in the study area until circa 9 ka, as suggested by seasonal precipitation distributions reconstructed by Williams from the White Pond pollen record of Watts (see Leigh, 2008, Fig. 5), increased summer and fall runoff from tropical storms provides a less plausible explanation for greater bankfull discharge during the terminal Pleistocene than other possible sources.

The 17–11 ka interval spans a timeframe when nearly every component of Earth's climate system experienced large-scale change (Clark et al., 2012), and attribution of hydrologic conditions in the southeastern US during this period involves considerable uncertainty (Leigh, 2008). At present, the paleoclimate of the region is still too poorly understood to definitively identify which driver or combination of drivers was responsible for greater channel-forming discharge during the terminal Pleistocene, and the competing alternative hypotheses discussed above remain to be tested. Paleoenvironmental proxy studies targeting identification of moisture sources for the region during this time period may help to resolve such questions and would be a potentially fruitful area of future research.

Interestingly, the three mega-meander channels that exhibit the largest paleo to modern discharge ratios (Congaree, Pee Dee, and Neuse River sites) have the most northerly drainage areas of the rivers evaluated in this study. Upstream of field sites, these basins are mainly contained away from the coast in the Piedmont and the inner Coastal Plain of North and South Carolina. As a consequence, they may have been more subject than the southerly sites to paleoenvironmental conditions that increased regional moisture and runoff, like intensification of frontal precipitation, snowmelt discharge, and/or rain on frozen ground. Russell et al. (2009) observe that plant and vertebrate remains indicate a warm-to-cool gradient existed within southeastern North America from peninsular Florida to Cape Hatteras (35°N) during the LGM and that a comparable but shorter temperature gradient likely occurred from the Atlantic Coast to the Southern Appalachian Mountains. The persistance of such a gradient, as climatic conditions ameliorated through the terminal Pleistocene, could account for the paleohydrological differences between northerly versus southerly sites observed in this study. However, given the limited number of paleochannels evaluated here, more mega-meanders from around the Southeast need to be examined before within-region variation in paleodischarge can be clearly assessed.

Paleomeanders resembling those in the study area are common along many rivers of northern Europe, where formerly braided channels developed large, meandering patterns in response to the afforestation, reduced sediment yields, increased bank stability, and more regular discharge regimes that accompanied climatic warming at the end of the Pleistocene (Starkel et al., 2015; Kasse et al., 2005; Vandenberghe et al., 1994). Relative to smaller Holocene channels, European terminal Pleistocene paleomeanders conveyed greater discharges that probably resulted from a combination of factors, including: continued influence of a pronounced snowmelt runoff season, high surface runoff due to persisting permafrost, ice jam floods, lower evapotranspiration, and, in some locations, higher precipitation (Kasse et al., 2010; Huisink, 1997; Kozarski, 1991; Rotnicki, 1991; Borisova et al., 2006; Sidorchuk et al., 2001). Paleochannels of comparable morphology and age also occur in the Great Lakes region of the United States, where greater discharge has been attributed to a high regional water table caused by melting of the Laurentide Ice Sheet and/or meltwater lake drainage (Arbogast et al., 2008). In contrast to these examples, the relatively low latitude catchments of the southeastern Coastal Plain did not receive glacial meltwater and were not influenced by widespread, continuous permafrost during the terminal Pleistocene. Instead, the large bankfull flows and oversized channel dimensions of mega-meanders appear to reflect response to more subtle changes in regional hydrology and sediment yield that were related to climatic and vegetation conditions that occurred in the study area during this time. Large meander development in the Atlantic Coastal Plain was probably facilitated by the fact that, from a systems perspective, rivers in the region appear to be situated in close proximity to a channel pattern threshold that enhances their sensitivity to changes in bedload sediment supply, bank stability, and discharge-driven fluctuations in stream power (Leigh et al., 2004). Such susceptibility to climate forcing in fluvial systems near threshold crossings has been recently discussed by Phillips (2010) and recognized by others (Vandenberghe et al., 1994; Kasse et al., 2003; Thomas, 2008).

The Oconee and Congaree mega-meanders, which respectively last functioned as active channels at or shortly before 12.1–12.5 and 11.8–12.1 ka, add to a regional dataset that indicates rivers in the study area did not revert to braiding during the Younger Dryas cold period of 12.7–11.5 ka (Leigh, 2006). This is compatible with the view of Kneller and Peteet (1999) that Younger Dryas cooling in eastern North America may have been weakly expressed or absent at locations south of 38°N latitude. Alternatively, if drier conditions observed in central Florida during this time (Willard et al., 2007) also existed at locations further to the north, as suggested by hydrogen isotope data from Jones and Singletary Lakes in the North Carolina Coastal Plain (Lane et al., 2018), the climatic shift may not have been of sufficient duration or magnitude to result in a channel pattern change.

5.3. Relationships between paleochannel cross-section shape and discharge

Given that mega-meanders conveyed bankfull flows at least twice as large as those of modern channels, one might wonder how paleobankfull discharge compares to present-day overbank flood magnitudes on rivers in the study area. Among the six study sites, best estimates of mega-meander bankfull discharge vary between two and four times larger than modern bankfull flows (Table 8). These results place paleobankfull discharge within the size range of two- to five-year recurrence interval floods on present-day rivers (Fig. 7, Table 9). Modern flood frequencies illustrate where this magnitude of discharge would fall within the present flow regime: that is, if a discharge of equivalent magnitude to mega-meander bankfull flow were to occur in the modern fluvial system, instead of representing an event with an approximately 99 to 90% annual exceedance probability (i.e., the modern bankfull discharge, see Table 8), it would equate to a flow with a 50 to 20% chance of being equaled or exceeded in any given year. Thus, while representing a larger, lower frequency event than the present bankfull discharge, mega-meander bankfull flow would nonetheless translate to a high frequency overbank flood within the annual series on modern rivers that most workers would regard as a relatively low magnitude event.

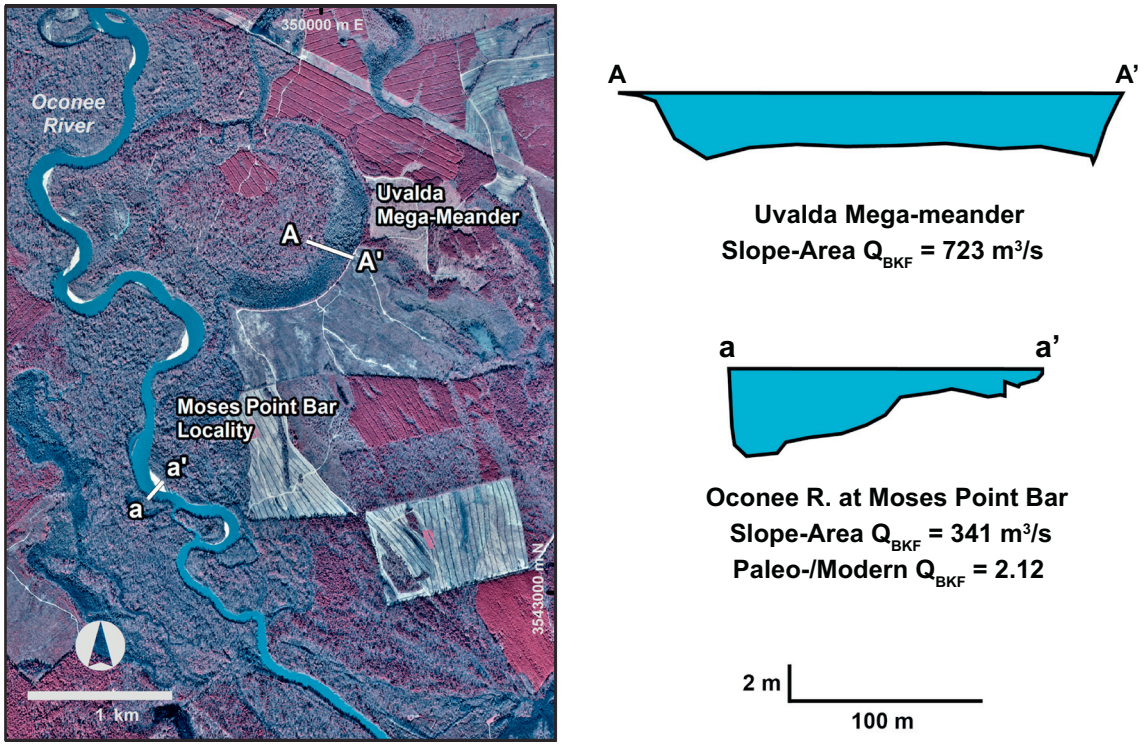

Fig. 8. Comparison of mega-meander and modern channel cross-sections of the Oconee River, Georgia. Bankfull discharge (Q_{BKF}) estimates by the slope-area method and the ratio of paleo to modern discharge are shown. The aerial image is a 1 m digital orthophotograph registered to the North American Datum of 1983 and UTM grid zone 17. The site vicinity corresponds to location 3A in Fig. 1.

Considering that mega-meanders dwarf modern rivers on aerial imagery (Figs. 3A–F and 8), with channel widths and radii of curvature that are up to five times greater than those of present-day channels in some cases (e.g., Figs. 3E and 9), it may seem surprising that paleo-bankfull discharge was not much larger. However, the relatively modest discharge magnitude conveyed by mega-meanders at the bankfull stage is attributable to basic parameters that influence open-channel flow. Because all available evidence indicates that mega-meanders had channel gradients about 50% steeper than their modern channel counterparts (Tables 2, 4, and 8), it is unlikely that paleodischarge values reflect underestimation of channel slope. It is also unlikely that overestimation of channel roughness produces a low-biased appraisal of discharge, given that the paleodischarge estimates presented here incorporate a wide range of Manning's *n* values (0.030–0.045) that well represent the lower range of possible roughness that could have been associated with mega-meanders. The modest discharge of mega-meanders is instead thought to reflect their wide, shallow cross-sectional shape, which is characterized by 1) a high width-to-depth ratio and correspondingly reduced hydraulic radius, and 2) a cross-sectional area (and thus a channel capacity) that is relatively modest in comparison to channel width.

The relationship between channel shape and paleodischarge can be better appreciated by examining the cross-sectional morphology of mega-meander channels. Mega-meanders do not constitute an enlarged version of the modern channel form; in contrast, they have a cross-sectional morphology that is distinctly different from that of modern rivers in the study area (Fig. 8, Supplementary Figs. 1–5). Stratigraphic cross-sections reveal that mega-meanders were wide and shallow, with an average width-to-depth ratio over four times greater than that of modern channels (Tables 7 and 8). As a consequence of this cross-sectional geometry, five of the six mega-meanders examined have hydraulic radii lower than those of their modern channel counterparts, while the average hydraulic radius among all mega-meanders is 21% lower than that of modern cross-sections (Tables 7 and 8). The hydraulic radius is expressed by cross-sectional area divided by the wetted perimeter, and it quantifies a channel's hydraulic efficiency by providing a measure of how much contact there is between flow and the channel boundary (Charlton, 2008). Morphological data indicate that mega-meanders had a proportionally greater length of their boundary in contact with flow than do modern rivers. As a result, the

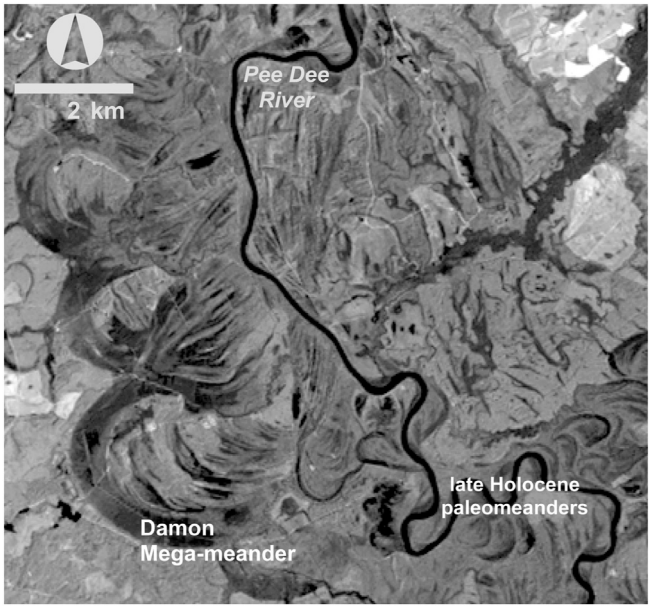

Fig. 9. Landsat image (band 4) of late Holocene paleomeanders within the floodplain of the Pee Dee River valley in the vicinity of the Damon mega-meander site. Note their morphological similarity with the modern river. The UTM NAD 83 Zone 17 coordinates for the center of this image are 616,156 m E and 3,810,640 m N.

paleochannels experienced increased frictional energy losses that reduced their flow velocity relative to what would be expected for a deeper cross-sectional channel morphology of equivalent width.

In addition to reducing the hydraulic radius of paleochannels, the wide, shallow shape of mega-meanders also limited their cross-sectional area. Together, these aspects of channel hydraulics, along with slope and boundary roughness, constrained the magnitude of in-channel flow that mega-meanders could accommodate. For a given river, this point can be illustrated by comparing mega-meander versus modern channel cross-sections that have been normalized by bankfull width. To facilitate this comparison, modern cross-sections were enlarged to a width equivalent to that of their respective counterpart paleomeander, using the same multiplier for width and depth so the enlarged cross-sections retain their original shapes. Although enlarged modern channels would have smaller roughness values at the bankfull stage owing to their greater depth, hypothetical cross-sections were assigned slope and Manning's n values equivalent to those of their counterpart mega-meander for ease of comparison. Results are given in Supplementary Table 1. For the five rivers where mega-meander and modern channels exhibit the greatest contrast in cross-sectional form (Ogeechee, Congaree, Black, Pee Dee, and Neuse), hypothetical enlarged modern channels have cross-sectional areas, hydraulic radii, and flow velocities that are respectively 3.7 to 7.6, 3.6 to 7.0, and 1.3 to 3.7 times larger than those of their mega-meander counterparts. Bankfull discharges for these hypothetical channels are ~9 to 28 times larger than mega-meander paleodischarge estimates (~14 to 114 times larger than present day bankfull flood sizes) and represent values that equal or exceed the estimated magnitude of the modern 500-year flood at paleochannel field sites. The greater discharge exhibited by enlarged modern channels in comparison to mega-meanders demonstrates the influence that cross-section size and shape exert on the magnitude of flow a channel can accommodate, other factors being equal. Despite having large planform dimensions, mega-meanders were restricted to carrying relatively modest flows at the bankfull stage by a wide, shallow cross-sectional shape, that reduced the hydraulic radius of paleochannels, limited cross-sectional area, and decreased the magnitude of in-channel flow that could be conveyed relative to what one would expect for a channel of comparable width with a more modern-like cross-sectional form.

5.4. Influence of historical impacts on paleo versus modern channel comparisons

Both impoundments and land use change have altered water and sediment delivery to rivers in the study area during the last 200 years (see Section 2.3). One might wonder to what extent present-day channels reflect historical changes to discharge and sediment supply and if the magnitude of change has been large enough to limit the value of contemporary systems as a comparative baseline for evaluating differences in paleodischarge relative to modern “natural” conditions.

With respect to impacts from impoundments, in a nationwide analysis that included nine rivers from the eastern United States, Graf (2006) found that one of the most important downstream hydrologic effects of very large ($\geq 1.2\ km^3$ storage capacity) dams in the region has been the reduction of annual peak discharges. However, for two of the four impounded rivers evaluated in the present paper, the impact of regulation on the size of high frequency peak flows appears to be small. On the Oconee River, Hess and Stamey (1992) note that the limited flood storage capacities of its major impoundments, Lake Oconee and Sinclair Reservoir (both located in the Piedmont), do not materially affect higher frequency annual peak discharges within the Coastal Plain reach of the river. In a hydrologic study of the Congaree River floodplain, Conrads et al. (2008) found that the Saluda Dam, the impoundment thought to be most responsible for the decrease in flood peaks on the Congaree since 1930, has only resulted in a 6.0 to 7.4% reduction in discharge for the two-, five-, and 10-year recurrence interval floods during this time. The authors attributed reduction in peak flows to climatic variability rather than dam operation. Thus, four of the six drainages examined here (the Oconee, Congaree, and undammed Ogeechee and Black Rivers) have not experienced large reductions in the magnitude of high frequency peak flows due to regulation.

Impoundment does appear to have reduced the magnitude of high frequency annual peaks on the Neuse River, whereas the impact of regulation on flood peaks of the Pee Dee River is more difficult to evaluate. Regulation patterns on the Pee Dee exhibit sufficient consistency to allow flood frequency estimation for the post-dam period from 1912 to present, but the record of unregulated flows downstream of the river's major impoundments is too short to permit reliable analysis for the pre-dam interval (Feaster et al., 2009, p. 36). Nonetheless, a high degree of similarity between the modern Pee Dee River and late Holocene paleomeanders (Fig. 9) suggests that any channel changes resulting from flow regulation have been small relative to the large differences in channel size and shape between mega-meanders, like the Damon paleochannel, and the present-day river. On the Neuse River in the vicinity of the Moccasin Creek mega-meander, published flood frequency estimates for USGS gage #02089000 near Goldsboro, NC exhibit respective decreases of 18.9, 11.5, and 6.2%, for the two-, five-, and 10-year recurrence interval discharges for the post-dam interval from 1981 to 2006 relative to the unregulated period of 1930–1980 (Weaver et al., 2009).

Although Atlantic drainages of the southeastern Coastal Plain have experienced historical fluctuations in water and sediment discharge from both impoundments and land use change, as discussed above and in Section 2.3, such impacts are not well-represented in their large river channel forms. Leigh (2008) notes that human impacts appear to have had little effect on the channel morphology of large rivers in the southeastern US relative to Late Pleistocene and early Holocene climate-mediated changes in runoff and sediment yield. This conclusion is supported by aerial imagery of study area river valleys (Fig. 3), including the Pee Dee valley noted above (Fig. 9), which indicates that modern channels are nearly identical in size and shape to paleomeanders of the late Holocene. Such evidence suggests that channel change resulting from historical impacts has been minor in comparison to morphological differences between mega-meanders and modern channels. From this standpoint, we believe that the modern channels examined in this study provide a reasonable basis for approximating differences in discharge and channel morphology between mega-meanders and the contemporary fluvial system.

Given that morphological distinctions between modern and late Holocene prehistoric channels in the study area are relatively small, comparative analysis of mega-meanders and modern rivers also has interpretive value for evaluation of terminal Pleistocene versus late Holocene paleochannels. Late Holocene paleomeanders, like modern channels, probably conveyed discharges at the bankfull stage that were at most half the size of the channel-forming flows carried by their mega-meander counterparts. However, in cases where anthropogenic impacts resulted in enlargement of modern relative to prehistoric channels (e.g., incision through historical sediments, increased runoff from land use change, dam- or bridge-induced scour), the magnitude of difference in bankfull discharge between mega-meanders versus late Holocene rivers may have been larger than discharge differences between mega-meanders and the modern system. Further field-based analysis that evaluates the explicit paleohydrology of late Holocene paleomeanders is needed before this relationship can be characterized with greater precision.

5.5. Sedimentologic controls on mega-meander channel morphology

Schumm (1960) demonstrated that bed and bank material functions as an important control on alluvial channel shape, noting that channels with coarse-grained perimeters tend to have high width-to-depth ratios, while streams with high silt and clay percentages in their boundaries are typically narrow and deep. Ritter et al. (2006) indicate such

relationships result in part from sediment transport mechanics: coarse grained bedload is more efficiently conveyed through a wide, shallow channel, while suspended load is most efficiently transported in cross-sections with low width-to-depth ratios. In a study with particular bearing on the influence of sandy bedload on width-sediment-discharge relationships, Osterkamp (1980) reports that streams of similar discharge in the western US are narrowest where the load is composed entirely of silt and clay and increase in width with tractive movement of sand, attaining maximum widths in channels that carry only medium to coarse sand. This trend reversed as bed material enlarged from sand to gravel to boulder sizes due to armoring effects (Osterkamp, 1980). Knighton (1998) states such findings imply that rivers that transport large quantities of sand require wider channels than streams that convey other sediment types.

Cross-section shape is also influenced by the strength and stability of channel banks, which is in part dependent on the cohesion of bank materials as expressed by their silt and clay content (Knighton, 1998). Effects of bank cohesion on cross-section geometry have been documented for both irrigation canals and natural channels. Simons and Albertson (1963) indicate that stable canals with sandy banks exhibit greater wetted perimeters and greater widths than do channels in more cohesive materials, while Huang and Nanson (1998) note that banks characterized by low vegetation densities and less cohesive sediments yield wider, shallower cross-sections than highly cohesive banks that are densely vegetated. With such associations in mind, Blum et al. (1995) observe that the scatter in many modern data sets used to relate discharge to planform meander geometry (Carlston, 1965; Dury, 1965) may reflect differences in bank material, with above average channel widths, meander wavelengths, and radii of curvature for a given discharge resulting from a lack of bank-stabilizing muds, and below average values reflecting more clay-rich, cohesive floodplain settings.

Given contemporary understanding of sedimentologic controls on alluvial channel morphology, in addition to larger than modern bankfull flows, it appears that the exceptionally large widths and radii of curvature of mega-meander channels also reflect a lack of fine-grained vertical accretion facies on paleomeander floodplains; a sediment discharge regime characterized by large quantities of bedload sand; and the influence of these factors on bed and bank composition and channel shape. Mega-meandering planforms were established near the end of the Pleistocene, following a late Wisconsin phase of sand-bed braiding and valley aggradation circa 30–17 ka. The channel pattern shift from braided to meandering is thought to represent river response to the onset of warmer, more moist climatic conditions, which drove afforestation and decreased upland sediment yield, while simultaneously stabilizing river banks with vegetation and causing incision beneath braided floodplains (Leigh, 2006, 2008). The distinctive, scrolled floodplains of terminal Pleistocene mega-meanders, which are underlain by large volumes of lateral accretion sand but comparatively smaller amounts of fine-grained vertical accretion deposits (Fig. 3, this paper; Leigh, 2006), confirm that mega-meanders transported large volumes of bedload sediment. This suggests that the large paleomeanders represent a transitional meandering planform that remained heavily influenced by large quantities of bedload sand following the sand-bed braiding of the 30–17 ka interval (Leigh, 2006, 2008).

An important source for this sandy bedload appears to have been sand from the braided terraces themselves, which was deposited by braided rivers that were aggrading their valleys in response to accelerated erosion and greater sediment yield from catchment uplands during late Wisconsin time (Leigh et al., 2004). Lateral incision of mega-meanders into braided terrace deposits at many regional localities (this paper; Leigh, 2006), indicates that the paleomeanders were actively eroding and reworking this sandy sediment when they functioned as river channels. Furthermore, Leigh et al. (2004) document that braided terrace remnants are widespread along small, medium, and large rivers in the Atlantic Coastal Plain of Georgia and the Carolinas, so the deposits would have been available as a potential sediment source of regional extent susceptible to reworking by terminal Pleistocene rivers. Such a geomorphic and sedimentologic context would readily satisfy the conditions required to yield the wide, shallow sand-bed channels typical of mega-meanders, given current understanding of relationships between sediment supply, bank material composition, and channel morphology. From a luminescence dating perspective, reworking of late Wisconsin braided terrace sediments by mega-meanders also could have easily resulted in the deposition of mixed populations of well- and poorly bleached quartz grains on paleomeander point bars, which would account for the older MAM estimates derived from OSL-dated scroll bar sands at some sites (see Section 5.1).

The scrolled mega-meandering planform of terminal Pleistocene channels may also reflect the influence of a paleoflood regime characterized by overbank flooding that was either less frequent or of shorter duration than in the Holocene, given the relative lack of vertical accretion facies associated with terminal Pleistocene mega-meanders in comparison to later meandering forms (Leigh, 2008). However, lower volumes of vertical accretion sediment on terminal Pleistocene floodplains may alternatively reflect that lateral migration of mega-meanders was so rapid that thick vertical accretion packages failed to accumulate (Leigh, 2008). Regardless, reduced quantities of fine-grained, overbank sediment on terminal Pleistocene floodplains would have resulted in less cohesive banks that favored wider channels and larger meander dimensions than those of later meandering forms.

One might wonder if the slopes of mega-meander channels, which, like the gradients of braided channels of the late Wisconsin interval (Leigh et al., 2004), appear to have been larger than those of modern rivers, also contributed to the sandy, scrolled pattern of terminal Pleistocene mega-meanders. The larger than modern slopes of these channels, which were graded to lower sea levels on the now submerged continental shelf, may have resulted in enhanced stream power and thereby greater capacity to transport bedload sediment. However, slope was probably not a primary driver responsible for the transitional, sandy scrolled mega-meander pattern, given that Leigh et al. (2004) indicate that modern floodplain gradients and 2-year discharges already place present-day large Coastal Plain rivers within the field of sand-bed braided streams of Kellerhals (1982) and in close proximity to the classic boundary line between braided and meandering streams of Leopold and Wolman (1957).

Considering that rivers in the study area continued to transport large quantities of sandy bedload during the terminal Pleistocene, one might also question why channels of this interval did not simply remain braided. The best explanation for the transition to meandering appears to be that, in addition to reducing upland sediment yield relative to late Wisconsin conditions, climate-driven afforestation also stabilized river banks with vegetation (Leigh, 2006). Nonetheless, scattered eolian dunes blown from sandy scroll bars on the interiors of some mega-meander bends (Fig. 3E) indicate that riparian environments of the terminal Pleistocene were probably less densely vegetated than those of the Holocene along southeastern rivers, especially on the point bar sides of paleochannels.

An increased caliber of bedload might be expected for Pleistocene rivers with larger-than-modern width-to-depth ratios and steeper slopes, but bed sediment sizes for mega-meander and modern channels are similar, consisting mainly of sand in the 0.25–2.0 mm range with some gravels (Section 4.1, Table 3, Figs. 3–4). Leigh et al. (2004) observed similar grain sizes for the bedload of late Wisconsin braided paleochannels in the study area and also report no difference in bed sediment size between Late Pleistocene and modern channels. Such findings indicate that, while the abundance of bedload supplied to rivers in the study area has clearly fluctuated during the late Quaternary, as shown by the present study and others (Leigh et al., 2004; Leigh, 2008), the size of bedload has remained relatively consistent. As indicated above, mega-meanders reworked large quantities of sandy bedload from late Wisconsin braided terrace deposits, and similarities

in bed sediment size among Late Pleistocene and modern rivers may to some extent reflect more limited reworking of sandy Pleistocene alluvium by Holocene and modern channels. The similar sandy bed textures of Late Pleistocene and modern channels is also attributable to the influence of source material on sediment load, as the primary upland sediment sources for rivers in the region (sandy surficial deposits in the Coastal Plain and saprolite in the Appalachian Piedmont; Leigh, 2008) both produce sediments containing large proportions of sand.

Blum et al. (1995) provide a model of channel formation for the "Deweyville" meander scars of the Gulf Coast that stresses the influence of bank composition and stability on channel morphology and argues against greater flood magnitudes as an explanation for the large paleomeanders. Although some workers infer much larger than modern channel-forming discharges for Deweyville paleochannels (Gagliano and Thom, 1967; Alford and Holmes, 1985; Sylvia and Galloway, 2006), Blum et al. (1995) argue that the large Deweyville channels represent hydraulic adjustments to a lack of bank-stabilizing muds that resulted from an absence of overbank floods during OIS 4–2. They contend that the smaller dimensions of Holocene Gulf Coast rivers simply reflect the presence of thick, bank-stabilizing muds that have accumulated in response to the more pronounced overbank flood regime that is characteristic of Holocene climatic conditions of the Texas Gulf Coast. In contrast, results of the present study indicate that the channel geometry of mega-meanders of the southeastern Atlantic Coastal Plain represents the influence of *both* sediment discharge regime on bed and bank material *and* greater bankfull flow magnitudes, rather than the effects of channel boundary sediment composition alone.

5.6. Paleochannels and late Quaternary sea-level change

Given the low elevations of study sites, one might wonder to what extent mega-meander paleochannels were influenced by late Quaternary sea-level change. Eustatic fluctuations lowered the base level of rivers in the southeastern Atlantic Coastal Plain during the Late Pleistocene, especially during the LGM when sea-level was 125 m lower than present (Balsillie and Donoghue, 2004). However, eustatic effects on fluvial systems in the region are not readily apparent > 60 to 80 km upstream of the coast and are limited to a thin mantle of Holocene sediments deposited during sea-level rise and river valley back-filling (Leigh, 2008). These sediments onlap and bury Late Pleistocene fluvial terraces within 60–80 km of the coast, including surfaces associated with mega-meandering and braided channel forms (e.g., the Qp3 and Qp2 alloformations depicted in Fig. 2), that were graded to lower sea-levels on the now submerged continental shelf. Similar limited upstream range of eustatic influence has been observed for rivers in the neighboring Gulf Coastal Plain (Otvos, 2005; Blum and Aslan, 2006), and it appears to be the result of 1) terrestrial sediment flux that overwhelmed any headward incision due to base-level lowering and 2) the width and gradient of the continental shelf, which confined the most pronounced base level effects on river channels to the outermost shelf and continental slope (Leigh, 2008). The continental shelf was exposed and functioned as an extension of the lower Coastal Plain during much of the Late Pleistocene, and its great width (> 100 km, see Fig. 1) positioned knickpoints and incised valleys far eastward, on the outer shelf and continental slope (Leigh, 2008). Modest incision (< 30 m) on the now-submerged inner continental shelf (Baldwin et al., 2006; Boss et al., 2002; Hine and Snyder, 1985) suggests that channel gradients changed little as rivers traversed the lower Coastal Plain onto the emergent shelf, probably owing to the similar gradients of the two surfaces, and this also likely inhibited upstream propagation of incision into areas landward of the modern shoreline (Leigh, 2008).

For most of the terminal Pleistocene, when mega-meanders were functioning as active river channels, base level was rising, as sea level increased by a cumulative 60 m from approximately −100 to −40 masl between circa 17 and 12 ka (Balsillie and Donoghue, 2004). However, paleochannel field sites are situated 80 (Black R.) to 150 (Congaree R.) km inland of the present-day shoreline, and positioned in their respective valleys well above the upstream limits of onlapping backfill associated with Holocene sea-level rise. This location would have placed mega-meanders even farther landward from paleoshoreline positions experiencing rising base levels during the terminal Pleistocene, within inland sectors of fluvial systems that were insulated from eustatic changes occurring at the time. Thus, the impact of eustatic fluctuation on mega-meander paleochannels would have been small, and their unusual channel morphology appears to reflect climate-mediated increases to bankfull discharge and the influence of a sandy sediment regime and lack of cohesive bank material on channel shape (as discussed in Sections 5.2 and 5.5), rather than a response to rising base levels at the end of the Pleistocene. This conclusion is consistent with findings from previous studies in the region, which indicate that eustasy played a subordinate role to climate as a forcing mechanism of channel change on southeastern Atlantic Coastal Plain rivers during the late Quaternary (Leigh and Feeney, 1995; Leigh et al., 2004; Leigh, 2006, 2008).

5.7. Methodological implications

Our findings underscore the importance of reconstructing paleochannel cross-sectional dimensions and slope when estimating discharge for infilled paleomeanders. This approach reduces uncertainties surrounding paleochannel cross-sectional area, gradient, and boundary composition that are inherent to studies that lack subsurface data and rely upon regression equations to retrodict discharge from planform meander dimensions (e.g. Williams, 1988).

Observations from the southeastern Atlantic Coastal Plain have implications for discharge estimation for paleomeanders in comparable alluvial environments, including the Deweyville paleochannels of the US Gulf Coast, for which paleodischarge estimates have been based mainly on planform meander geometry (Alford and Holmes, 1985; Gagliano, 1991; Sylvia and Galloway, 2006) and channel-forming discharge remains a subject of debate (Blum and Aslan, 2006). Subsurface investigations that provide high resolution channel cross-sections and adequate constraint on slope may help to resolve longstanding questions about past variation in discharge and its relationship to late Quaternary environmental change in these settings.

6. Conclusions

Terminal Pleistocene mega-meanders of the southeastern Atlantic Coastal Plain represent channel-forming discharges that were at least double the magnitude of modern bankfull flows in the region. Larger than modern bankfull discharge appears to have been driven by seasonally wetter conditions resulting from dynamic changes to regional precipitation and runoff that occurred in association with global warming at the end of the Pleistocene. Although the precise climatic controls responsible for greater discharge during this time period are poorly known, several mechanisms are possible, including: increased frontal precipitation resulting from enhanced concentration of storm-track associated moisture on the region during winter and spring; the existence of a pronounced snowmelt season or rain on frozen ground events, which may have intensified spring runoff; greater summer and fall rainfall caused by increased frequency of landfalling tropical storms; or higher levels of effective precipitation. At present, the paleoclimatic and hydrologic conditions of the study area during the terminal Pleistocene involve considerable uncertainty, and the precise cause of the larger bankfull flows of this interval stands as an important question in the paleoenvironmental history of the southeastern United States that remains to be solved. Notably, mega-meanders provide an example of pronounced channel morphological response to late Quaternary climatic change from a low latitude setting that did not experience glacial meltwater inputs or widespread periglacial

landscape conditions. This response was probably facilitated by the fact that Coastal Plain rivers appear to be positioned near a channel pattern threshold that enhances their sensitivity to variations in bank stability, bedload sediment supply, and discharge-driven fluctuations in stream power.

Paleodischarges presented in this study are significant, not only because they indicate larger than modern bankfull flow for the study area during the terminal Pleistocene, but also because they place limits on the magnitude of channel-forming discharge that large paleomeanders in the region represent. Best estimates indicate mega-meanders conveyed bankfull flows no more than two to four times greater than those of modern channels. In terms of magnitude, this places paleobankfull discharge within the range of two- to five-year recurrence interval flood sizes in the modern gaged flood regime for comparison. Thus, while representing larger than modern channel-forming flows, the unusually large widths, radii of curvature, and wavelengths of the paleomeanders appear to have been maintained by a relatively modest discharge, equivalent to that of the 50 to 20% annual exceedance probability flood in the present-day flow regime. Although mega-meanders had exceptionally large planimetric dimensions, they were restricted to conveying discharges of relatively modest magnitude at the bankfull stage by a wide, shallow geometry that reduced the hydraulic radius of paleochannels and limited channel cross-sectional area.

Within the broader context of the late Quaternary evolution of fluvial systems in the region, scrolled terminal Pleistocene mega-meanders likely represent a transitional meandering planform that was still influenced by large volumes of sandy bedload sediment immediately following the braided, sand-bed channels of the late Wisconsin interval (ca. 30–17 ka). In addition to reflecting greater bankfull flows, the large planform dimensions and distinctive scroll-work of these paleomeanders appear to be the product of a lack of fine-grained vertical accretion facies on paleomeander floodplains, a sediment discharge regime that transported large amounts of bedload sand, and the influence of these factors on channel boundary composition, bank stability, and channel shape.

Results from this research highlight the value of field-based reconstruction of channel cross-sectional dimensions and slope when determining discharge for infilled paleomeanders in the study area and comparable alluvial environments. Such an approach decreases uncertainties related to paleochannel cross-sectional area, gradient, and boundary composition that are inherent to studies without subsurface data that instead solely rely upon regression equations to estimate discharge from planform meander geometry.

Supplementary data to this article can be found online at https://doi.org/10.1016/j.palaeo.2018.07.002.

Acknowledgments

This work was supported by a National Geographic Society Committee for Research and Exploration grant (#8850-10), the Educational Component of the U.S. Geological Survey's National Cooperative Mapping Program (EDMAP grant #G11 AC20162), and the University of Georgia Graduate School's Dean's and Dissertation Completion Awards. The Kennesaw State University College of Humanities and Social Sciences, Office of the Provost and Vice President for Academic Affairs, and Graduate College provided funding for equipment used to conduct laboratory analyses. Jessie Hughes, Zack Sanders, Sean Cameron, Dustin Menhart, Amy Woodell, Jason Rumfelt, Matt Mitchelson, and Mike Grimaldi served as field assistants. Christopher Sipes performed particle size and LOI analyses. We thank David Shelley of Congaree National Park and the numerous private landowners who provided access to field sites. This study benefited from modern channel cross-sections provided by Anthony J. Gotvald and Timothy Lanier, respectively of the Georgia and South Carolina offices of the USGS South Atlantic Water Science Center; the South Carolina Department of Transportation; and Thomas E. Langan of the North Carolina Floodplain Mapping Program. However, the design and conclusions of this research remain exclusively those of the authors. An earlier draft of this paper benefited from the thoughtful comments of two anonymous reviewers.

References

Aitken, M.J., 1985. Thermoluminescence Dating. Academic Press (359 pp.).
Aitken, M.J., 1998. An Introduction to Optical Dating. Oxford University Press (280 pp.).
Aldridge, B.N., Garrett, J.M., 1973. Roughness Coefficients for Stream Channels in Arizona: United States Geological Survey Open-File Report. (87 pp.).
Alford, J.J., Holmes, J.C., 1985. Meander scars as evidence of major climate changes in Southeast Louisiana. Ann. Assoc. Am. Geogr. 75, 395–403.
Alley, R.B., 2000. The younger Dryas cold interval as viewed from Central Greenland. Quat. Sci. Rev. 19, 213–226.
Andrews, E.D., 1979. Scour and fill in a stream channel, East Fork River, Western Wyoming. United States Geological Survey Professional Paper 1117. (49 pp.).
Arbogast, A.F., Bookout, J.R., Schrotenboer, B.R., Lansdale, A., Rust, G.L., Bato, V.A., 2008. Post-glacial fluvial response and landform development in the upper Muskegon River valley in North-Central Lower Michigan, U.S.A. Geomorphology 102, 615–623.
Arcement, G.J., Schneider, V.R., 1989. Guide for selecting Manning's roughness coefficients for natural channels and flood plains. Water Supply Paper 2339. United States Geological Survey (38 pp.).
Autin, W.J., Burns, S.F., Miller, B.J., Saucier, R.T., Snead, J.I., 1991. Quaternary geology of the Lower Mississippi Valley. In: Morrison, R.B. (Ed.), Quaternary Nonglacial Geology; Coterminous U.S., Boulder, CO. K-2. Geological Society of America, the Geology of North America, pp. 547–582.
Baldwin, W.E., Morton, R.A., Putney, T.R., Katuna, M.P., Harris, M.S., Gayes, P.T., Driscoll, N.W., Denny, J.F., Schwab, W.C., 2006. Migration of the Pee Dee River system inferred from ancestral paleochannels underlying the South Carolina Grand Strand and Long Bay inner shelf. Geol. Soc. Am. Bull. 118, 533–549.
Balsillie, J.H., Donoghue, J.F., 2004. High Resolution Sea-Level history for the Gulf of Mexico Since the Last Glacial Maximum. Report of Investigations. Vol. 103 Florida Geological Survey, Tallahassee (66 pp.).
Bard, E., 2002. Abrupt climate changes over millennial time scales: climate shock. Phys. Today 55 (12), 32–38.
Barnes, H.H., 1967. Roughness characteristics of natural channels. U.S. In: Geological Survey Water-Supply Paper. 1849 U.S. Government Printing Office, Washington, D.C (213 pp.).
Benson, M.A., Dalrymple, Tate, 1967. General field and office procedures for indirect discharge measurements: United States Geological Survey Techniques of Water-Resources Investigations. In: Book 3, Chapter Al, (30 pp.).
Berger, G.W., 1990. Effectiveness of natural zeroing of the thermoluminescence in sediments. J. Geophys. Res. 95 (12), 12,375–12,397.
Berger, G.W., Luternauer, J.J., 1987. Preliminary field work for thermoluminescence dating studies at the Fraser River delta, British Columbia. In: Geological Survey of Canada Paper 87/IA, pp. 901–904.
Blum, M.D., Aslan, A., 2006. Signatures of climate vs. sea-level change within incised valley fill successions: quaternary examples from the Texas Gulf Coast. Sediment. Geol. 190, 177–211.
Blum, M.D., Morton, R.A., Durbin, J.M., 1995. "Deweyville" terrace and deposits of the Texas Gulf Coastal Plain. 45. Gulf Coast Association of Geological Societies Transactions, pp. 53–60.
Borisova, O., Sidorchuk, A., Panin, A., 2006. Palaeohydrology of the Seim River basin, Mid-Russian Upland, based on palaeochannel morphology and palynological data. Catena 66, 53–73.
Boss, S.K., Hoffman, C.H., Cooper, B., 2002. Influence of fluvial processes on the Quaternary geologic framework of the continental shelf, North Carolina, USA. Mar. Geol. 183, 45–65.
Bourke, M.C., Child, A., Stokes, S., 2003. Optical age estimates for hyper-arid fluvial deposits at Homeb, Namibia. Quat. Sci. Rev. 22, 1099–1103.
Bridge, J.S., 2003. Rivers and Floodplains: Forms, Processes, and Sedimentary Record. Blackwell Publishing, Malden, MA (491 pp.).
Brook, G.A., Luft, E.R., 1987. Channel pattern changes along the lower Oconee River, Georgia, 1805/7 to 1949. Phys. Geogr. 8, 191–209.
Carlston, C.A., 1965. The relation of free meander geometry to stream discharge and its geomorphic implications. Am. J. Sci. 263, 864–885.
Carson, E.C., Knox, J.C., Mickelson, D.M., 2007. Response of bankfull flood magnitudes to Holocene climate change, Uinta Mountains, northeastern Utah. Geol. Soc. Am. Bull. 119 (9/10), 1066–1078.
Charlton, R., 2008. Fundamentals of Fluvial Geomorphology. Routledge, New York, NY (234 pp.).
Clark, P.U., Shakun, J.D., Baker, P.A., Bartlein, P.J., Brewer, S., Brook, E., Carlson, A.E., Cheng, H., Kaufman, D.S., Liu, Z., et al., 2012. Global climate evolution during the last deglaciation. Proc. Natl. Acad. Sci. U. S. A. 109, E1134–E1142.
Conrads, P.A., Feaster, T.D., Harrelson, L.G., 2008. The effects of the Saluda Dam on the surface-water and groundwater hydrology of the Congaree National Park flood plain, South Carolina. US Geol. Surv. Sci. Investig. Rep. 2008–5170, 58.
Cowan, W.L., 1956. Estimating hydraulic roughness coefficients. Agric. Eng. 37 (7), 473–475.
Cunningham, A.C., Wallinga, J., 2010. Selection of integration time intervals for quartz OSL decay curves. Quat. Geochronol. 5, 657–666.
Dobur, J.C., Noel, J., Hatcher, K.J., 2005. A climatological assessment of flood events in Georgia. In: Proceedings of the 2005 Georgia Water Resources Conference. Institute

of Ecology, The University of Georgia, Athens, Georgia.
Duller, G.A.T., 1999. Luminescence Analyst computer programme V2.18. Department of Geography and Environmental Sciences, University of Wales, Aberystwyth (528 pp.).
Duller, G.A.T., 2008. Single-grain optical dating of Quaternary sediments: why aliquot size matters in luminescence dating. Boreas 37, 589–612.
Dury, G.H., 1965. Theoretical implications of underfit streams. US Geol. Surv. Prof. Pap. 452-C, C1–C43.
Dury, G.H., 1976. Discharge prediction, present and former, from channel dimensions. J. Hydrol. 30, 219–245.
Dury, G.H., 1985. Attainable standards of accuracy in the retrodiction of paleodischarge from channel dimensions. Earth Surf. Process. Landf. 10, 205–213.
Feaster, T.D., Gotvald, A.J., Weaver, J.C., 2009. Magnitude and frequency of rural floods in the southeastern United States, 2006-volume 3, South Carolina: U.S. Geological Survey Scientific Investigations Report. 2009–5156 (226 pp.).
French, H.M., Millar, S.W.S., 2014. Permafrost at the time of the Last Glacial Maximum (LGM) in North America. Boreas 43, 667–677.
French, H.M., Demitroff, M., Newell, W.L., 2009. Past permafrost on the Mid-Atlantic Coastal Plain, Eastern United States. Permafr. Periglac. Process. 20, 285–294.
Frey, D.G., 1951. Pollen succession in the sediments of Singletary Lake, North Carolina. Ecology 32, 518–533.
Gagliano, S.M., 1991. Late quaternary interval Deweyville interval superfloods. In: Gulf Coast Association of Geological Societies Transactions. 41. pp. 298.
Gagliano, S.M., Thom, B.G., 1967. Deweyville terrace, Gulf and Atlantic Coasts. Louisiana State University, Coastal Studies Bulletin. 1. pp. 23–41.
Galbraith, R.F., Roberts, R.G., 2012. Statistical aspects of equivalent dose and error calculation and display in OSL dating: an overview and some recommendations. Quat. Geochronol. 11, 1–27.
Galbraith, R.F., Roberts, R.G., Laslett, G.M., Yoshida, H., Olley, J.M., 1999. Optical dating of single and multiple grains of quartz from Jinmium rock shelter, northern Australia, part 1, experimental design and statistical models. Archaeometry 41, 339–364.
Gamble, D.W., Meentemeyer, V.G., 1997. A synoptic climatology of extreme unseasonable floods in the southeastern United States, 1950–1990. Phys. Geogr. 18, 496–524.
Goman, M., Leigh, D.S., 2004. Wet early to middle Holocene conditions on the upper Coastal Plain of North Carolina, USA. Quat. Res. 61, 256–264.
Gotvald, A.J., Feaster, T.D., Weaver, J.C., 2009a. Magnitude and frequency of rural floods in the southeastern United States, 2006-volume 1, Georgia. US Geol. Surv. Sci. Investig. Rep. 2009-5043, 120.
Gotvald, A.J., Feaster, T.D., Weaver, J.C., 2009b. Flood-frequency applications tool for use on streams in Georgia, South Carolina, and North Carolina, Version 1.3. Available at. http://pubs.usgs.gov/sir/2009/5156/, Accessed date: 3 June 2013.
Graf, W.L., 2006. Downstream hydrologic and geomorphic effects of large dams on American rivers. Geomorphology 79, 336–360.
Guccione, M.J., Burford, M., Kendall, J., Nunn, C., Odhiambo, B., Porter, D., Shepherd, S., 2001. Channel fills of all scales from the Mississippi River alluvial valley. In: Abstracts with Programs - Geological Society of America. 33. pp. 356.
Hadley, J.B., Goldsmith, R., 1963. Geology of the Eastern Great Smoky Mountains, NorthCarolina and Tennessee. In: U.S. Geological Survey Professional Paper. vol. 349-B Government Printing Office, Washington, D.C.
Happ, S.C., 1945. Sedimentation in South Carolina Piedmont valleys. Am. J. Sci. 243, 113–126.
Heiri, O., Lotter, A.F., Lemcke, 2001. Loss on ignition as a method for estimating organic and carbonate content in sediments: reproducibility and comparability of results. J. Paleolimnol. 25, 101–110.
Herschy, R.W., 1985. Streamflow Measurement. Elsevier, London (553 pp.).
Hess, G.W., Stamey, T.C., 1992. Annual peak discharges and stages for gaging stations in Georgia, through September 1990. In: U.S. Geological Open-File Report, pp. 92–113.
Hine, A.C., Snyder, S.W., 1985. Coastal lithosome preservation: evidence from the shoreface and inner continental shelf off Bogue Banks, North Carolina. Mar. Geol. 63, 307–330.
Hoogsteen, M.J.J., Lantinga, E.A., Bakker, E.J., Groot, J.C.J., Tittonell, P.A., 2015. Estimating soil organic carbon through loss on ignition: effects of ignition conditions and structural water loss. Eur. J. Soil Sci. 66, 320–328.
Howard, A.J., Macklin, M.G., Bailey, D.W., Mills, S., Andreescu, R., 2004. Late-glacial and Holocene river development in the Teleorman Valley on the southern Romanian Plain. J. Quat. Sci. 19, 271–280.
Huang, H.Q., Nanson, G.C., 1998. The influence of bank strength on channel geometry: an integrated analysis of some observations. Earth Surf. Process. Landf. 23, 865–876.
Huisink, M., 1997. Late-glacial sedimentological and morphological changes in a lowland river in response to climatic change: the Maas, southern Netherlands. J. Quat. Sci. 12, 209–223.
Hupp, C.R., Schenk, E.R., Kroes, D.E., Willard, D.A., Townsend, P.A., Peet, R.K., 2015. Patterns of floodplain sediment deposition along the regulated lower Roanoke River, North Carolina: annual, decadal, centennial scales. Geomorphology 228, 666–680.
Hussey, T.C., 1993. A 20,000-Year History of Vegetation and Climate at Clear Pond, Northeastern South Carolina. M.S. Thesis. University of Maine, Orono, Maine, USA.
Indorante, S.J., Follmer, L.R., Hammer, R.D., Koenig, P.G., 1990. Particle-size analysis by a modified pipette procedure. Soil Sci. Soc. Am. J. 54, 560–563.
Ingram, R.L., 1971. Sieve analysis. In: Carver, R.E. (Ed.), Procedures in Sedimentary Petrology. Wiley, New York, pp. 49–67.
Ivester, A.H., 1999. Quaternary Geology of Inland Dunes in Georgia, USA. PhD Dissertation. University of Georgia, Athens.
Ivester, A.H., Brookes, M.J., Taylor, B.E., 2007. Sedimentology and ages of Carolina bay sand rims. Abstracts of the southeastern section of the 56th annual meeting of the southeastern section of the Geological Society of America in savannah, GA. Geol. Soc. Am. Abstr. Programs 39 (2), 5.
Ivester, A.H., Leigh, D.S., 2003. Riverine dunes on the coastal plain of Georgia, U.S.A. Geomorphology 51, 289–311.
Ivester, A.H., Leigh, D.S., Godfrey-Smith, D.I., 2001. Chronology of inland eolian dunes on the coastal plain of Georgia, USA. Quat. Res. 55, 293–302.
Jackson, C.R., Martin, J.K., Leigh, D.S., West, L.T., 2005. Historical agricultural sediments in a southeastern piedmont river; a multi millennial legacy. J. Soil Water Conserv. 60, 298–310.
Kasse, C., Vandenberghe, J., Van Huissteden, J., Bohncke, S.J.P., Bos, J.A.A., 2003. Sensitivity of Weichselian fluvial systems to climate change (Nochten Mine, eastern Germany). Quat. Sci. Rev. 22, 2141–2156.
Kasse, C., Hoek, W.Z., Bohncke, S.J.P., Konert, M., Weijers, J.W.H., Cassee, M.L., Van der Zee, R.M., 2005. Late Glacial fluvial response of the Niers-Rhine (western Germany) to climate and vegetation change. J. Quat. Sci. 20, 377–394.
Kasse, C., Bohncke, S.J.P., Vandenberghe, J., Gábris, G., 2010. Fluvial style changes during the last glacial-interglacial transition in the middle Tisza valley (Hungary). Proc. Geol. Assoc. 121, 180–194.
Kellerhals, R., 1982. Effect of river regulation on channel stability. In: Hey, R.D., Bathhurst, J.C., Thorne, C.R. (Eds.), Gravel-Bed Rivers. Wiley, Chichester, pp. 685–705.
Kerr, W.C., 1881. On the action of frost in the arrangement of superficial earthy material. Am. J. Sci. 21, 345–358.
Kneller, M., Peteet, D., 1999. Late-glacial to early Holocene climate changes from a central Appalachian pollen and macrofossil record. Quat. Res. 51, 133–147.
Knighton, D., 1998. Fluvial Forms and Processes: A New Perspective. Arnold, London (383 pp.).
Knox, J.C., 1985. Responses of floods to Holocene climate change in the Upper Mississippi Valley. Quat. Res. 23, 287–300.
Kozarski, S., 1983. River channel adjustment to climatic change in west central Poland. In: Gregory, K.J. (Ed.), Background to Palaeohydrology. Wiley, Chichester, pp. 355–374.
Kozarski, S., 1991. Warta – a case study of a lowland river. In: Starkel, L., Gregory, K.J., Thomes, J.B. (Eds.), Temperate Palaeohydrology. Wiley, New York, pp. 189–215.
LaMoreaux, H.K., Brook, G.A., Knox, J.A., 2009. Late Pleistocene and Holocene environments of the Southeastern United States from the stratigraphy and pollen content of a peat deposit on the Georgia Coastal Plain. Palaeogeogr. Palaeoclimatol. Palaeoecol. 280, 300–312.
Lane, C.S., Taylor, A.K., Spencer, J., Jones, K.B., 2018. Compound-specific isotope records of late-Quaternary environmental change in southeastern North Carolina. Quat. Sci. Rev. 182, 48–64.
Lea, D.W., Pak, D.K., Peterson, L.C., Hughen, K.A., 2003. Synchroneity of tropical and high-latitude Atlantic temperatures over the last glacial termination. Science 301, 1361–1364.
Leigh, D.S., 2006. Terminal Pleistocene braided to meandering transition in rivers of the Southeastern USA. Catena 66, 155–160.
Leigh, D.S., 2007. Geomorphology and Related Archaeological Site Burial Potential at Fort Stewart and Hunter Army Airfield, Georgia. In: University of Georgia Geomorphology Laboratory Research Report 4, (Athens, GA).
Leigh, D.S., 2008. Late Quaternary climates and river channels of the Atlantic Coastal Plain, Southeastern USA. Geomorphology 101, 90–108.
Leigh, D.S., Feeney, T.P., 1995. Paleochannels indicating wet climate and lack of response to lower sea level, Southeast Georgia. Geology 23, 687–690.
Leigh, D.S., Srivastava, P., Brook, G.A., 2004. Late Pleistocene braided rivers of the Atlantic Coastal Plain, USA. Quat. Sci. Rev. 23, 65–84.
Leopold, L.B., Wolman, M.G., 1957. River Channel Patterns: Braided, Meandering, and Straight. US Geological Survey Professional Paper 282-B. US Government Printing Office, Washington, pp. 39–85.
Leopold, L.B., Wolman, M.G., Miller, J.P., 1964. Fluvial Processes in Geomorphology. W.H. Freeman, San Francisco (544 pp.).
Magilligan, F.J., Nislow, K.H., 2005. Changes in hydrologic regime by dams. Geomorphology 71, 61–78.
Magilligan, F.J., Stamp, M.L., 1997. Historical land-cover change and hydrogeomorphic adjustment in a small Georgia watershed. Ann. Assoc. Am. Geogr. 87, 614–635.
Markey, B.G., Bøtter-Jensen, L., Duller, G.A.T., 1997. A new flexible system for measuring thermally and optically stimulated luminescence. Radiat. Meas. 27, 83–90.
Meade, R.H., Yuzyk, T.R., Day, T.J., 1990. Movement and Storage of Sediment in Rivers of the United States and Canada. In: Wolman, M.G., Riggs, H.C. (Eds.), Surface Water Hydrology. Geological Society of America, the Geology of North America, Vol. O-1, Boulder, pp. 255–280.
Murray, A.S., Wintle, A.G., 2000. Luminescence dating of quartz using an improved single-aliquot regenerative-dose protocol. Radiat. Meas. 32, 57–73.
North American Commission on Stratigraphic Nomenclature, 2005. North American stratigraphic code. AAPG Bull. 89 (11), 1547–1591.
Osterkamp, W.R., 1980. Sediment-morphology relations of alluvial channels. In: Proceedings of the Symposium on Watershed Management. 1980. American Society of Civil Engineers, Boise, pp. 188–199.
Otvos, E.G., 2005. Numerical chronology of Pleistocene coastal plain and valley development; extensive aggradation during glacial low sea-levels. Quat. Int. 135, 91–113.
Patterson, G.G., Speiren, G.K., Whetson, B.H., 1985. Hydrology and its effects on vegetation in Congaree National Monument, South Carolina. US Geological Survey Water Resources Investigation Report. pp. 85–4256.
Peel, M.C., Finlayson, B.L., McMahon, T.A., 2007. Updated world map of the Köppen-Geiger climate classification. Hydrol. Earth Syst. Sci. Discuss. 11, 1633–1644.
Péwé, T.L., 1983. The periglacial environment in North America during Wisconsin time. In: Porter, S.C. (Ed.), The Late Quaternary Environments of the United States. Vol. 1. University of Minnesota Press, Chicago, pp. 157–189.
Phillips, J.D., 1993. Pre- and post-colonial sediment sources and storage in the lower Neuse River basin, North Carolina. Phys. Geogr. 14, 272–284.

Phillips, J.D., 1997. Human agency, Holocene Sea level, and floodplain accretion in coastal plain rivers. J. Coast. Res. 13 (3), 854–866.
Phillips, J.D., 2010. Amplifiers, filters and geomorphic responses to climate change in Kentucky rivers. Clim. Chang. 103, 571–595.
Prescott, J.R., Hutton, J.T., 1994. Cosmic ray contributions to dose rates for luminescence and ESR dating: large depths and long-term time variations. Radiat. Meas. 23, 497–500.
Reinfelds, I., Bishop, P., 1998. Palaeohydrology, palaeodischarges and palaeochannel dimensions: research strategies for meandering alluvial rivers. In: Benito, G., Baker, V.R., Gregory, K.J. (Eds.), Palaeohydrology and Environmental Change. Wiley, New York 368.
Rich, F.J., Vega, A., Vento, F.J., 2011. Evolution of late Pleistocene-Holocene climates and environments of St. Catherines Island and the Georgia Bight. In: Bishop, G.A., Rollins, H.B., Thomas, D.H. (Eds.), Geoarchaeology of St. Catherines Island, Georgia. Anthropological Papers of the American Museum of Natural History. 94. pp. 67–78.
Rittenour, T.M., 2008. Luminescence dating of fluvial deposits: applications to geomorphic, palaeoseismic and archaeological research. Boreas 37, 613–635.
Ritter, D.F., Kochel, R.C., Miller, J.R., 2006. Process Geomorphology, Fourth Edition. Waveland Press, Long Grove, pp. 560.
Rotnicki, K., 1991. Retrodiction of palaeodischarges of meandering and sinuous alluvial rivers and its palaeohydrologic implications. In: Starkel, L., Gregory, K.J., Thomes, J.B. (Eds.), Temperate Palaeohydrology. Wiley, New York, pp. 431–470.
Rotnicki, K., Borówka, R., 1985. Definition of subfossil meandering palaeochannels. Earth Surf. Process. Landf. 10, 215–225.
Russell, D.A., Rich, F.J., Schneider, V., Lynch-Stieglitz, J., 2009. A warm thermal enclave in the Late Pleistocene of the Southeastern United States. Biol. Rev. 84, 173–202.
Schumm, S.A., 1960. The Shape of Alluvial Channels in Relation to Sediment Type: Erosion and Sedimentation in a Semiarid Environment. US Geological Survey Professional Paper 352-B. US Government Printing Office, Washington, pp. 17–30.
Sidorchuk, A., 2003. Floodplain sedimentation: inherited memories. Glob. Planet. Chang. 39, 13–29.
Sidorchuk, A., Borisova, O., Panin, A., 2001. Fluvial response to the Late Valdai/Holocene environmental change on the East European Plain. Glob. Planet. Chang. 28, 303–318.
Simons, D.B., Albertson, M.L., 1963. Uniform water conveyance channels in alluvial material. Trans. Am. Soc. Civ. Eng. 128, 65–107.
Soil Survey Division Staff, 1993. Soil Survey Manual. U.S. Department of Agriculture Handbook 18. U.S. Government Printing Office, Washington, D.C., USA (437 pp.).
Srivastava, P., Brook, G.A., Marais, E., Morthekai, P., Singhvi, A.K., 2006. Depositional environment and OSL chronology of the Homeb silt deposits, Kuiseb River, Namibia. Quat. Res. 65, 478–491.
Starkel, L., Michczyńska, D.J., Gębica, P., Kiss, T., Panin, A., Perşoiu, I., 2015. Climatic fluctuations reflected in the evolution of fluvial systems of Central-Eastern Europe (60-8 ka cal BP). Quat. Int. 388, 97–118.
Stuiver, M., Reimer, P.J., Reimer, R.W., 2016. CALIB 7.1 [WWW program] at. http://calib.org, Accessed date: 15 December 2016.
Suther, B.E., 2013. Stratigraphy, paleohydrology, and soil variability in Late Quaternary river valleys of the southeastern Atlantic Coastal Plain, USA. In: PhD Dissertation. University of Georgia, Athens.
Swezey, C.S., Schultz, A.P., Alemán-González, W., Bernhardt, C.E., Doar III, W.R., Garrity, C.P., Mahan, S.A., McGeehin, J.P., 2013. Quaternary aeolian dunes in the Savannah River valley, Jasper County, South Carolina, USA. Quat. Res. 80, 250–264.
Swezey, C.S., Fitzwater, B.A., Whittecar, G.R., Mahan, S.A., Garrity, C.P., Aleman Gonzalez, W.B., Dobbs, K.M., 2016. The Carolina Sandhills: quaternary eolian sand sheets and dunes along the updip margin of the Atlantic coastal plain province, southeastern United States. Quat. Res. 86, 271–286.
Sylvia, J.P.M., Galloway, W.E., 2006. Morphology and stratigraphy of the late Quaternary lower Brazos valley: implications for paleoclimate, discharge, and sediment delivery. Sediment. Geol. 190, 159–175.
Thomas, M.F., 2008. Understanding the impacts of late Quaternary climate change in tropical and sub-tropical regions. Geomorphology 101, 146–158.
Trimble, S.W., 1974. Man-induced soil erosion in the southern piedmont 1700–1970. Soil Conservation Society of America, Ankeny, Iowa (180 pp.).
United States Department of Agriculture, Natural Resources Conservation Service, 2016. Field Indicators of Hydric Soils in the United States, Version 8.0. L.M. In: Vasilas, G.W. Hurt, Berkowitz, J.F. (Eds.), USDA, NRCS, in cooperation with the National Technical Committee for Hydric Soils, (45 pp.).
Vandenberghe, J., Kasse, C., Bohncke, S., Kozarski, S., 1994. Climate-related river activity at the Weichselian-Holocene transition: a comparative study of the Warta and Maas Rivers. Terra Nova 6 (5), 476–485.
Viau, A.E., Gajewski, K., Sawada, M.C., Fines, P., 2006. Millennial-scale temperature variations in North America during the Holocene. J. Geophys. Res. 111, D09102. https://doi.org/10.1029/2005JD006031.
Walter, R.C., Merritts, D.J., 2008. Natural streams and the legacy of water-powered mills. Science 319, 299–304.
Watts, W.A., 1980. Late-Quaternary vegetation history at white pond on the inner coastal-plain of South-Carolina. Quat. Res. 13, 187–199.
Weaver, J.C., Feaster, T.D., Gotvald, A.J., 2009. Magnitude and frequency of rural floods in the southeastern United States, through 2006-volume 2, North Carolina: U.S. Geological Survey Scientific Investigations Report. 2009–5158 (111 pp.).
Webb, T.I.I.I., Shuman, B., Williams, J.W., 2004. Climatically forced vegetation dynamics in eastern North America during the late Quaternary Period. pp. 459–478. In: Gillespie, A.R., Porter, S.C., Atwater, B.F. (Eds.), "The Quaternary Period in the United States," Developments in Quaternary Science vol. 1 (series editor Rose, J.). Elsevier, Amsterdam (584 pp.).
Whiting, P.J., 2003. Flow measurement and characterization. In: Kondolf, M., Piegay, H. (Eds.), Tools in Fluvial Geomorphology. John Wiley and Sons, Ltd, West Sussex, England, pp. 323–346.
Willard, D.A., Bernhardt, C.E., Brooks, G.R., Cronin, T.M., Edgar, T., Larson, R., 2007. Deglacial climate variability in central Florida, USA. Palaeogeogr. Palaeoclimatol. Palaeoecol. 251, 366–382.
Williams, G.P., 1988. Paleofluvial estimates from dimensions of former channels and meanders. In: Baker, V.R., Kochel, R.C., Patton, P.C. (Eds.), Flood Geomorphology. John Wiley and Sons, New York, pp. 357–376.
Wójcicki, K.J., 2006. The oxbow sedimentary subenvironment: its value in palaeogeographical studies as illustrated by selected fluvial systems in the upper Odra catchment, southern Poland. The Holocene 16 (4), 589–603.